# Active Faulting Geometry and Stress Pattern Near Complex Strike-Slip Systems Along the Maghreb Region: Constraints on Active Convergence in the Western Mediterranean

Abdelkader Soumaya, Noureddine Ben Ayed, Mojtaba Rajabi, Mustapha Meghraoui, Damien Delvaux, Ali Kadri, Moritz Ziegler, Said Maouche, Ahmed Braham

AGU100 ADVANCING EARTH AND SPACE SCIENCE

Tectonics

RESEARCH ARTICLE
10.1029/2018TC004983

Special Section:
Geodynamics, Crustal and Lithospheric Tectonics, and active deformation in the Mediterranean Regions (A tribute to Prof. Renato Funiciello)

# Active Faulting Geometry and Stress Pattern Near Complex Strike-Slip Systems Along the Maghreb Region: Constraints on Active Convergence in the Western Mediterranean

**Abdelkader Soumaya[1,2], Noureddine Ben Ayed[3], Mojtaba Rajabi[4], Mustapha Meghraoui[5], Damien Delvaux[6], Ali Kadri[3], Moritz Ziegler[7,8], Said Maouche[9], and Ahmed Braham[2]**

[1]Faculty of Sciences Tunis, University of Manar, Tunis, Tunisia, [2]National Office of Mines, Tunisia, [3]Faculty of Sciences Bizerte, University of Carthage, Tunis, Tunisia, [4]Australian School of Petroleum, University of Adelaide, Adelaide, South Australia, Australia, [5]Institut de Physique du Globe de Strasbourg (UMR 7516), Strasbourg, France, [6]Earth Sciences Department, Royal Museum for Central Africa, Tervuren, Belgium, [7]Helmholtz Centre Potsdam, German Research Centre for Geosciences GFZ, Potsdam, Germany, [8]Institute of Earth and Environmental Science, University of Potsdam, Potsdam, Germany, [9]CRAAG, Bouzareah-Alger, Algeria

**Key Points:**
- Maghreb region is characterized by different geometries of active strike-slip faults
- Present-day active contraction on western Africa-Eurasia boundary is accommodated by a combination of strike-slip and thrust faulting
- Second-order tectonic regime across Maghreb varies with clockwise rotation of $S_{Hmax}$ from east to west

**Correspondence to:**
A. Soumaya,
abdelkader.smeya@gmail.com

**Citation:**
Soumaya, A., Ben Ayed, N., Rajabi, M., Meghraoui, M., Delvaux, D., Kadri, A., et al. (2018). Active faulting geometry and stress pattern near complex strike-slip systems along the Maghreb region: Constraints on active convergence in the western Mediterranean. *Tectonics*, *37*, 3148–3173. https://doi.org/10.1029/2018TC004983

Received 18 JAN 2018
Accepted 10 AUG 2018
Accepted article online 23 AUG 2018
Published online 22 SEP 2018

**Abstract** The Maghreb region (from Tunisia to Gibraltar) is a key area in the western Mediterranean to study the active tectonics and stress pattern across the Africa-Eurasia convergent plate boundary. In the present study, we compile comprehensive data set of well-constrained crustal stress indicators (from single focal mechanism solutions, formal inversion of focal mechanism solutions, and young geologic fault slip data) based on our and published data analyses. Stress inversion of focal mechanisms reveals a first-order transpression-compatible stress field and a second-order spatial variation of tectonic regime across the Maghreb region, with a relatively stable $S_{Hmax}$ orientation from east to west. Therefore, the present-day active contraction of the western Africa-Eurasia plate boundary is accommodated by (1) E-W strike-slip faulting with reverse component along the Eastern Tell and Saharan-Tunisian Atlas, (2) a predominantly NE trending thrust faulting with strike-slip component in the Western Tell part, and (3) a conjugate strike-slip faulting regime with normal component in the Alboran/Rif domain. This spatial variation of the present-day stress field and faulting regime is relatively in agreement with the inferred stress information from neotectonic features. According to existing and newly proposed structural models, we highlight the role of main geometrically complex shear zones in the present-day stress pattern of the Maghreb region. Then, different geometries of these major inherited strike-slip faults and its related fractures (V-shaped conjugate fractures, horsetail splays faults, and Riedel fractures) impose their component on the second- and third-order stress regimes. Neotectonic and smoothed present-day stress map (mean $S_{Hmax}$ orientation) reveal that plate boundary forces acting on the Africa-Eurasia collisional plates control the long wavelength of the stress field pattern in the Maghreb. The current tectonic deformations and the upper crustal stress field in the study area are governed by the interplay of the oblique plate convergence (i.e., Africa-Eurasia), lithosphere-mantle interaction, and preexisting tectonic weakness zones.

## 1. Introduction

The complex architecture of the western Mediterranean domain (Figure 1) has originated from the slow oblique plate convergence between Africa and Eurasia (Dewey et al., 1989; Le Pichon et al., 1988), which has been active since the Late Cretaceous (Calais et al., 2003; DeMets et al., 1994; McClusky et al., 2003; Serpelloni et al., 2007). In the western Mediterranean, the diffuse plate boundary is characterized by an overall E-W trending line parallel to the coastal Maghreb region, from the Strait of Gibraltar to Tunisia (Buforn et al., 2004; Meghraoui & Pondrelli, 2013), which consequently displays a complex pattern of active deformation. The major strike-slip faults, interacting with thrust and fold systems (Meghraoui & Pondrelli, 2013), are formed on the site of ancient large Mesozoic and Oligo-Miocene basins with high-angle normal faults (Benaouali-Mebarek et al., 2006; Bracene & Frizon de Lamotte, 2002; Favre & Stamphli, 1992; Oldow et al. 1990; Piqué et al., 2002; Vially et al., 1994; Wildi, 1983). They played important roles in the structural evolution of the Maghreb region during the Tertiary time. Their Cenozoic and Quaternary reactivation generated a set of en echelon thrust folds and conjugate strike-slip faults (e.g., Ben Ayed, 1993; Meghraoui, 1988; Meghraoui

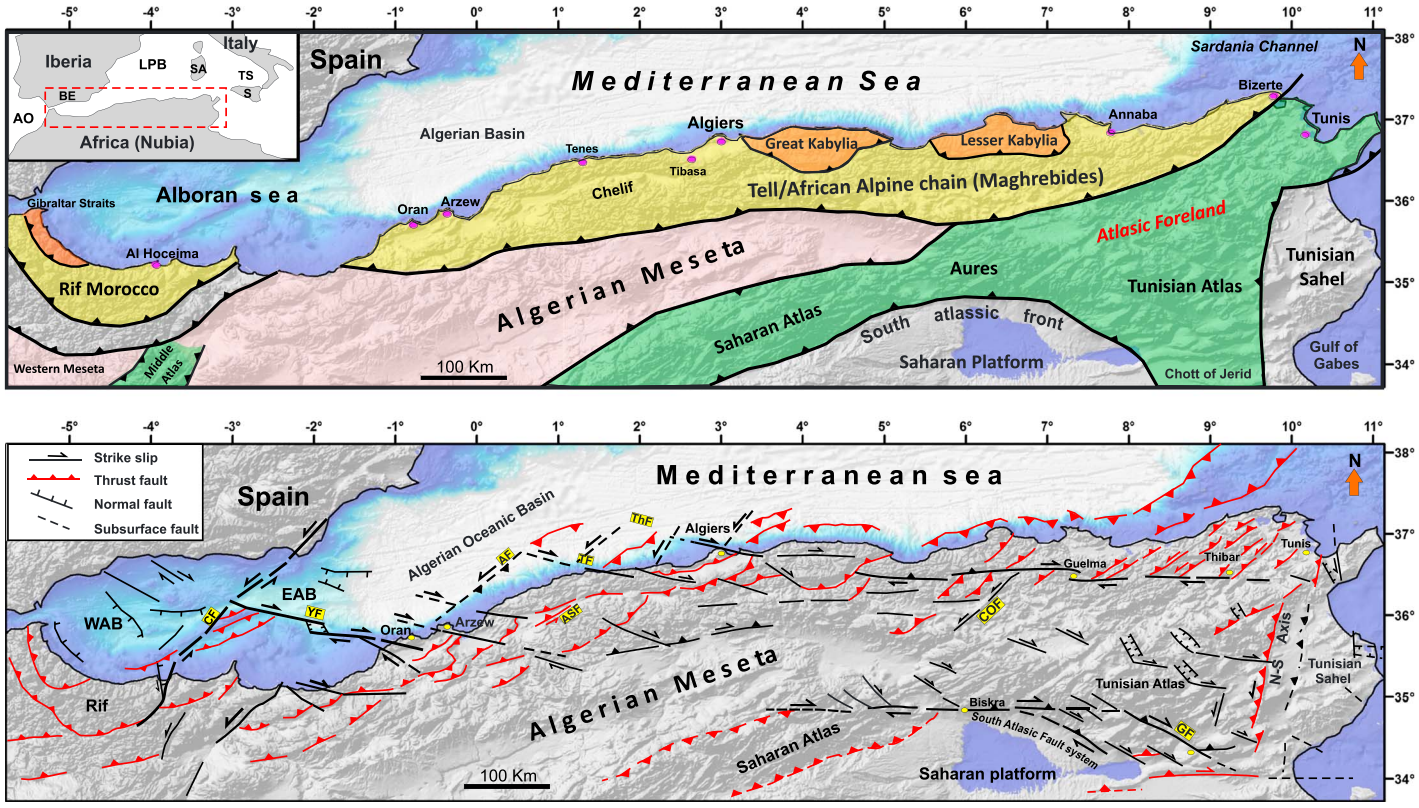


**Figure 1.** Simplified tectonic map showing the main geological and structural features of the Maghreb region. This map was established using Medaouri et al. (2014), Meghraoui et al. (1996), Leprêtre et al. (2018), Vially et al. (1994), Ben Ayed (1993), Domzig et al. (2009), Mauffret (2007), Martínez-García et al. (2011), Rabaute and Chamot-Rooke (2014), Yelles et al. (2009), and Medina (1995). Abbreviations are as follows: WAB: Western Alboran Basin, EAB: Eastern Alboran Basin, SAB: Southern Alboran Basin, CF:Chott fault, COF: Canstantine fault, THF: Thenia fault, TF: Ténes fault, AF: Arzew fault, ASF: Al Asnam fault, YF: Yusuf fault, CF: Carboneras fault zone, GF: Gafsa fault.

et al., 1996; Yielding et al., 1989) with different style and degree of deformation. This region is dominated by NW-SE to E-W right-lateral strike-slip faults and NE-SW left-lateral range-front thrust faults that cut the Tell/Rif (Maghrebides) and Atlasic belts (foreland). Subordinate NE-SW left-lateral strike-slip faults are also present. The seismic events and related stress distribution generated by these fault systems are distributed with an overall E-W trending and NW-SE shortening component along the Africa-Eurasia plate boundary (Ousadou et al., 2014).

In the last decade, numerous seismotectonic and neotectonic syntheses on local and regional scales have been published for the Maghreb area (e.g., Buforn et al., 2004; Mauffret, 2007; Meghraoui et al., 1986; Negredo et al., 2002; Ousadou et al., 2014; Palano et al., 2013; Pondrelli et al., 2006; Rebaï et al., 1992; Serpelloni et al., 2007; Soumaya et al., 2015). However, this region (i.e., Africa-Eurasia plate boundary) is still mostly described by a simplified compressive belt from Morocco to Sicily (Serpelloni et al., 2007). The combination of GPS measurements (e.g., Fadil et al., 2006; Nocquet, 2012; Palano et al., 2013), geodetic model (e.g., Serpelloni et al., 2007), moment tensor solutions (Pondrelli et al., 2006), and geophysics and paleomagnetic data (e.g., Aïfa et al., 1992; Balanyá et al., 2007) sustain the oblique convergence plates with counterclockwise rotation of Africa with respect to Eurasia (e.g., Meghraoui et al., 1996). The E-W crustal right-lateral faulting from Azores-Gibraltar to North Tunisia has played a key role in neotectonic and present-day strain deformation, with transpressive regime in North Africa (e.g., Buforn et al., 2004; Gomez et al., 2000; Morel & Meghraoui, 1996). The accommodation of maximum of convergence between Africa and Eurasia (Iberia) is along the Tell/Rif alpine chain at the upper crustal level, through thrusting above detachment systems, which are controlled by first-order shear zones (e.g., Meghraoui & Pondrelli, 2013, and references therein). GPS velocities show 4–5 mm/yr of shortening accommodated in Southern Spain and North Africa Alpine belt (Nocquet, 2012), namely, Maghrebides (Tell in Algeria and Tunisia and Rif in Morocco; Durand-Delga & Fontobé,

1980, and references therein). In addition, Calais et al. (2003) inferred up to 8-mm/yr convergence rates between Tunisia and Sicily.

This paper addresses different faulting geometry and stress pattern near the active strike-slip fault systems and related structures along the Africa-Eurasia convergent plate boundary in the Maghreb region. We compile well-constrained focal mechanisms and neotectonic stress data from published works and seismicity catalogs. With the completed database, we perform formal stress inversions on spatial subsets of the data in order to investigate the consistency of the first-order stress field and secondary stress pattern variations on studied strike-slip faults. Finally, we infer and discuss the key role exerted by various geometries of strike-slip fault systems, with newly proposed structural models on spatial pattern of strain rate fields in the Maghreb region.

## 2. Geodynamic and Tectonic Settings

Most of the established geodynamic studies used a slab retreat model to explain the tectonic evolution during the Cenozoic of the western Mediterranean area that includes fold-thrust belts and back-arc basins (e.g., Faccenna et al., 2004; Jolivet et al., 2009; Piromallo & Morelli, 2003; Royden, 1993; Wortel & Spakman, 2000). Since late Paleogene-Neogene, from northern Morocco to northern Sicily, contraction deformation has shifted from the old subduction domain to the margins of the two oceanic back-arc basins (Algerian-Provençal and Tyrrhenian Sea). The result of the slab retreat was the stripping off of the Alboran, Kabylie, Peloritan, and Calabria (AlKaPeCa) zones from the European margin (Alvarez et al., 1974; Bouillin, 1986; Frizon de Lamotte et al., 2000; Rémi Leprêtre et al., 2018; Wildi, 1983). Thus, the African Tethyan lithosphere subduction was at the origin of development of the complex orogenic belt, represented by the fold-thrust belt of Maghrebides and Atlas domains (e.g., Billi et al., 2011; Bracene & Frizon de Lamotte, 2002, 1983; Favre & Stampfli, 1992). In this setting, the main Maghreb tectonic features consist essentially of two different structural domains (Figure 1) including the Tell-Rif chain (Rif in Morocco and Tell in Algeria and Tunisia) or Maghrebides and the Atlas belt (foreland), which extends from Morocco to Tunisia, north of the Saharan platform (e.g., Bracene & Frizon de Lamotte, 2002; Durand-Delga & Fonboté, 1980).

The Maghrebides were considered as the Alpine chain of North Africa resulting from the closure of the Tethyan oceanic Basin (Auzende et al., 1973; Durand-Delga & Fontobé, 1980). It consists a Neogene pile of thrust sheets trending E-W with a significant curvature in the Rif, which swings from E-W in the its eastern part to N-S in the western part (Frizon de Lamotte et al., 2000; Rémi Leprêtre et al., 2018; Roure et al., 2012). During the lower Oligocene-Burdigalian, northward subduction and slab retreat of African oceanic lithosphere allowed the deposition of the Numidian flysch at the front of the Kabylides nappes (e.g., Essid et al., 2016; Frizon de Lamotte et al., 2000; Roure et al., 2012). The collision between AlKaPeCa and Africa occurred during the Langhian (e.g., Frizon de Lamotte et al., 2000; Jolivet & Faccenna, 2000; Rémi Leprêtre et al., 2018; Roure et al., 2012). During the Tortonian, the subducting slab break off accelerated the continental collision and occurred the uplift of the Tellian domain (e.g., Benaouali-Mebarek et al., 2006; Faccenna et al., 2004; Frizon de Lamotte et al., 2009; Roure et al., 2012; Soumaya et al., 2015). Since 8 to 2 Ma, a progressive compression and basin inversion has propagated in a scissor-like way from the west in Gibraltar arc (Alboran and Liguro-provencal) to the east in Tyrrhenian basins following a similar propagation of the cessation of the Tethyan subduction (e.g., Billi et al., 2011; Faccenna et al., 2004). In the Alboran Basin, the extensional regime keeps on going until the Messinian; when folding, strike slip tectonics and inversion of preexisting normal faults began in surrounding areas (e.g., Chalouan et al., 1997; Comas et al., 1992; Jolivet & Faccenna, 2000; Martínez-García et al., 2011; Meghraoui et al., 1986).

The Atlas system is an intraplate (i.e., intracontinental) high mountain belt originated during the Cenozoic Alpine collision that affected the African Margin (Piqué et al., 2002) in the location of a preexisting continental extensional Basins (e.g., Bracene & Frizon de Lamotte, 2002; Mattauer et al., 1977). It has been traditionally considered as intraplate in nature, distinguished from intercontinental mountain belts (i.e., the Alpine belts) by their distance from the collisional area and the lack of ophiolites, nappe structures, and metamorphism (Gomez et al., 2000). During late Eocene and middle late Miocene, a contractional regime has affected the entire intracontinental basin and surroundings domains that are generally estimated to have produced the main amount (almost 40 km) of intraplate shortening across the entire intracontinental basin (Benaouali-Mebarek et al., 2006). The South Atlas Front (SAF) constitutes the limit between Atlas Mountain

chain and the Sahara platform (Bracene & Frizon de Lamotte, 2002) that has apparently been reactivated during the Quaternary, particularly in Morocco during the 1960 Agadir earthquake (Meghraoui et al., 1996), and toward Tunisia (Soumaya et al., 2015; Vially et al., 1994, and references therein).

Since Quaternary, after the closure of Neogene basins under an oblique convergence trending NW-SE to N-S, the majority of preexisting weakness zones crossing Morocco, northern Algeria, and Tunisia are reactivated as strike slip and thrust faulting (e.g., Ben Ayed, 1993; Bracene & Frizon de Lamotte, 2002; Essid et al., 2016; Meghraoui & Pondrelli, 2013; Rebaï et al., 1992; Soumaya et al., 2015; Vially et al., 1994). Hence, the tectonic deformation of the Maghreb region along the Africa-Eurasia boundary is still strongly controlled by the inherited heterogeneous features, in particular the strike-slip fault systems and related compressive structures outlining a broad belt of diffuse moderate seismicity also called GALTEL along the plate boundary (Meghraoui et al., 1996).

## 3. Data and Methodology

### 3.1. Focal Mechanisms Background

A focal mechanism solution (FMS) describes the geometry and mechanism of the faulting during a given earthquake and is widely used in order to derive stress tensor distribution (Heidbach et al., 2016; Müller et al., 1992; Rajabi et al., 2017). The orientation of the maximum horizontal stress ($S_{Hmax}$) is derived from the principal strain axes (McKenzie, 1969). In order to study the pattern of seismotectonic deformation and establish detailed maps of stress orientations and tectonic regime in the study area, we compile the result of recent published studies (Heidbach et al., 2016; Ousadou et al., 2014; Palano et al., 2013; Soumaya et al., 2015). Hence, we complete and improve our database (Figure 2) that contains 200 single focal mechanism solutions, which are classified based on the World Stress Map nomenclature and quality ranking (Heidbach et al., 2016). In addition, the results of our formal stress inversion are also classified based on the World Stress Map ranking criteria (Figure 2). To classify the earthquake focal mechanisms according to the faulting types (i.e., strike slip, thrust, and normal) in our data set, we refer to the ternary diagram of Frohlich (1992). This diagram offers a manageable way to visualize the dominant style of faulting in a given region. We then discriminate strike-slip and normal fault seismic events as those having *P* and *B* axis plunges of less than 30° and thrust earthquakes as those having *T* axis plunges of less than 40°, respectively. The remaining FMS were defined as *others* (Figure 2).

Therefore, the sum of moment tensors or the strain axes resulting from cumulative moment tensor analyses (Figure 2) indicate strike-slip and reverse dominant style of faulting apart from some few normal events that are related to complex local fault geometry. In a global way, the E-W and NW-SE trending splays show right-lateral strike-slip mechanisms similar to the main strand, whereas antithetic NE-SW and N-S trending faults show reverse and left-lateral strike-slip motions, respectively.

### 3.2. Stress Inversion Methodology

To define the stress field, we invert focal mechanism solutions for the four stress parameters: the three principal stress axes orientations (maximum $\sigma 1$, intermediate $\sigma 2$, and minimum $\sigma 3$ compressive stresses) and the stress ratio $R = (\sigma 2 - \sigma 3/\sigma 1 - \sigma 3)$ with $0 \leq R \leq 1$. Formal stress inversion of focal mechanisms reduces the difference between the maximum shear stress and the slip direction of earthquakes (Bott, 1959; Gephart & Forsyth, 1984; Heidbach et al., 2016), which provides the most reliable information on the orientation of maximum horizontal stress (i.e., *A* and *B*) according to the World Stress Map quality ranking criteria (Heidbach et al., 2016; Zoback, 1992). In this study, we perform formal stress inversions of the available focal mechanisms, following the technique of TENSOR program (Delvaux & Sperner, 2003) and using the Win-Tensor program (Delvaux, 2012). According to the method described in Delvaux and Barth (2010), we minimize the composite function (F5) in Win-Tensor, which simultaneously minimizes the angular misfit between observed and modeled slip on the focal planes and favor slip on the focal planes by maximizing the resolved shear stress and minimizing the resolved normal stress. With this approach, we estimate the directions of the three principal stresses and the stress ratio *R*, which expresses the magnitude of $\sigma 2$ relative to the magnitude of $\sigma 1$ and $\sigma 3$. In addition of these four parameters, we obtain the true orientations of the horizontal principal stresses ($S_{Hmax}$ and $S_{hmin}$) according to Lund and Townend (2007). To map the faulting styles and relative stress regime across the study region, we

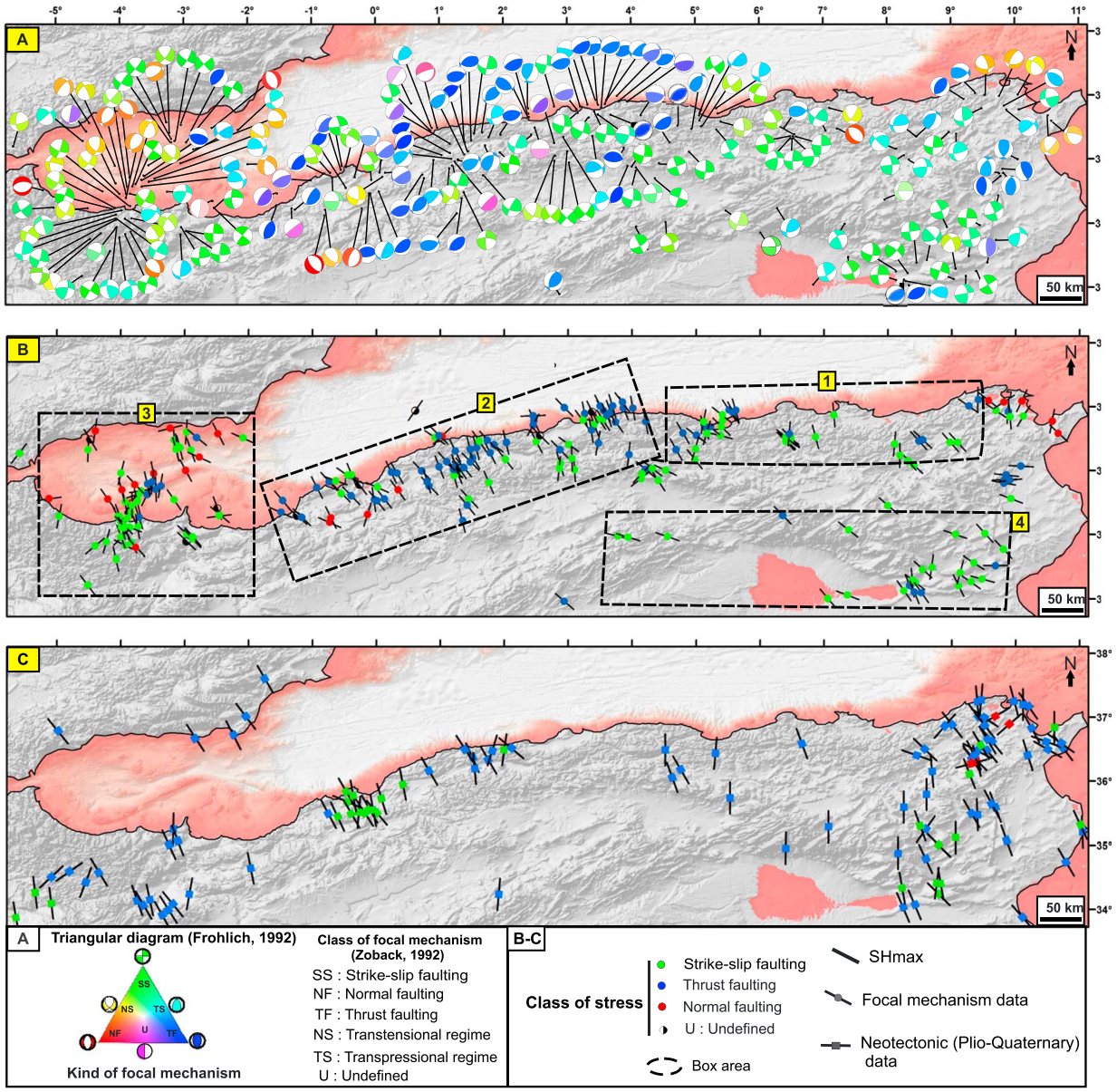


**Figure 2.** (a) Focal mechanism solution data (e.g., Harvard CMT; Heidbach et al., 2016) into boxes for stress inversion. (b) $S_{Hmax}$ axis of focal mechanism solution data represented into boxes; a color-coded central circle indicates the stress type. (c) Neotectonic (Plio-Quaternary period) $S_{Hmax}$ (Heidbach et al., 2016; Meghraoui, 1988; Morel & Meghraoui, 1996; Rebaï et al., 1992; Soumaya et al., 2016).

utilize the $R'$ stress ratio following Delvaux et al. (1997) that ranges from 0 (uniform horizontal extension with $S_V > S_{Hmax} = S_{hmin}$) to 1.5 (strike-slip faulting with $S_{Hmax} > S_V > S_{hmin}$) to 3 (uniform horizontal compression with $S_{Hmax} = S_{hmin} > S_V$). The tectonic stress regime index $R'$ is defined as

1. $R' = R$ for normal faulting regime
2. $R' = 2 - R$ for strike-slip faulting regime
3. $R' = 2 + R$ for reverse faulting regime

Computation of the standard deviations is based on the examination of all possible reduced stress tensors for a particular stress solution (Delvaux, 2012). The iterative inversion procedure is combined with data filtering in order to progressively remove the noncompatible data (those for which F5 $>$ 35) and filter the data set. The focal mechanism data are weighted according to the earthquake magnitude $M$ ($M_w$ when available). The weight of each datum is calculated as $10^M$. This way of working favors naturally the largest-magnitude events.

**Table 1**
*Stress Inversion Results (Parameters of the Stress Tensor and Stress Map)*

| Box | Domain | Magnitudes | *n* | Nt | n/nt | S1pl | S1az | S2pl | S2az | S3pl | S3az | *R* | *R*′ | $S_{Hmax}$ | $R_{eg}$ | $Q_{Rw}$ |
|---|---|---|---|---|---|---|---|---|---|---|---|---|---|---|---|---|
| 1 | Eastern Tell | All | 20 | 23 | 0,87 | 9 | 324 | 58 | 219 | 30 | 59 | 0,39 | 1.61 ± 0.19 | 146 ± 5.1 | SS | A |
| | | $M >= 4.5$ | 8 | 10 | 0,80 | 4 | 333 | 61 | 235 | 29 | 65 | 0,65 | **1.35 ± 0.23** | **154 ± 7.6** | **SS** | B |
| | | $M < 4.5$ | 12 | 13 | 0,92 | 12 | 313 | 9 | 45 | 75 | 172 | 0,24 | 2.24 ± 0.13 | 132 ± 9.0 | TF | B |
| 2 | Western Tell | All | 56 | 83 | 0,67 | 2 | 145 | 3 | 55 | 87 | 275 | 0,41 | 2.41 ± 0.20 | 145 ± 9.5 | TF | A |
| | | $M >= 4.5$ | 52 | 59 | 0,88 | 0 | 327 | 5 | 57 | 85 | 232 | 0,43 | **2.43 ± 0.21** | **147 ± 9.4** | **TF** | A |
| | | $M < 4.5$ | 14 | 24 | 0,58 | 2 | 326 | 56 | 60 | 34 | 235 | 0,26 | 1.74 ± 0.09 | 146 ± 5.1 | SS | B |
| 3 | Alboran-Rif | All | 38 | 62 | 0,61 | 18 | 347 | 71 | 184 | 5 | 79 | 0,7 | 1.30 ± 0.21 | 168 ± 10.6 | SS | A |
| | | $M >= 5.0$ | 16 | 17 | 0,94 | 17 | 325 | 71 | 165 | 6 | 56 | 0,51 | **1.49 ± 0.24** | **146 ± 7.5** | **SS** | A |
| | | $5.0 > M >= 4.5$ | 12 | 19 | 0,63 | 23 | 321 | 67 | 129 | 4 | 229 | 0,7 | 1.30 ± 0.10 | 140 ± 4.2 | SS | B |
| | | $M < 4.5$ | 18 | 26 | 0,69 | 25 | 1 | 63 | 207 | 11 | 96 | 0,57 | 1.43 ± 0.13 | 4 ± 2.5 | SS | B |
| 4 | Saharan-Tunisian Atlas | All | 26 | 31 | 0,84 | 9 | 317 | 70 | 200 | 18 | 50 | 0,34 | 1.66 ± 0.13 | 137 ± 6.2 | SS | A |
| | | $M >= 4.5$ | 14 | 19 | 0,74 | 10 | 317 | 68 | 201 | 19 | 50 | 0,35 | **1.65 ± 0.12** | **138 ± 6.9** | **SS** | B |
| | | $M < 4.5$ | 12 | 12 | 1,00 | 16 | 317 | 69 | 96 | 13 | 223 | 0,22 | 1.78 ± 0.17 | 136 ± 6.3 | SS | B |

*Note*. *n*: number of data used in stress tensor solution; nt: number of data in the subset; parameters of the reduced stress tensors: plunge (Pl), azimuth (Az) of the principal stress axes ($\sigma 1$, $\sigma 2$, and $\sigma 3$), stress ratio (*R* and *R*′) and its sigma 1 standard deviation, tectonic regime (TF: thrust fault; SS: strike-slip fault), and quality rank for the stress inversion of focal mechanisms (QRfm) as defined in the World Stress Map.

### 3.3. Stress Field

The study area of the Maghreb region is too large and the focal mechanisms too diverse in order to compute a unique first-order stress field for the entire region, and such result would be meaningless. We therefore explore whether these variations in stress regime correspond to lateral changes of the active second-order stress field and tectonic regime. We divided the group of focal mechanisms in four selected subsets according to a zonation in function of the major Maghreb strike-slip fault systems (Figure 2b). The results of stress inversion are given in Figure 7 and Table 1. The selected boxes cover the major active strike-slip fault systems of the study area and contain a sufficiently large number of focal mechanisms, which reflect both the stress regime and the orientation of the preexisting faults.

For each box, we first inverted the focal mechanisms for all the magnitudes; then for magnitude class with generally $M >= 4.5$ and $M < 4.5$, except for Box 3 with $M >= 5.0$, $5.0 > M >= 4.5$ and $M < 4.5$ (Table 1 and Figure 7). We consider that stress tensor inverted from the largest magnitude of focal mechanism earthquakes is more likely to represent the first-order stress field in the region, while those from the smallest magnitude would represent local stress deviations. In the Eastern Tell domain (Box 1), the largest-magnitude mechanisms (8 of 10 data) characterize a strike-slip stress regime ($R' = 1.35 \pm 0.23$), and the smallest mechanisms (12 of 13 data), a thrust faulting regime ($R' = 2.24 \pm 0.13$). Similarly, the horizontal principal compression ($S_{Hmax}$) is more sub-Meridian (N154°E ± 7.6°) for largest-magnitude mechanisms than for the smallest ones (N132°E ± 9.0°). Both sets use a large proportion of their representative data (80 and 92%) in the inversion.

The Western Tell domain (Box 2) displays an opposite situation, with thrust faulting ($R' = 2.43 \pm 0.21$) for the largest-magnitude earthquakes and strike-slip faulting ($R' = 1.74 \pm 0.09$) for the small and moderate magnitudes. Both stress tensors have a similar $S_{Hmax}$ (N147°E ± 9.4° and N146°E ± 5.1°), but the largest-magnitude focal mechanisms are more numerous (59) and a largest proportion of them is compatible with the stress inversion result (88% instead of 24% and 58%) for the small magnitudes.

Farther west, within the Alboran-Rif area (Box 3), the stress inversion gives significantly different results in function of the magnitude class. The entire database (62 data) gives a stress tensor with only 61% compatible data. In contrast, the largest-magnitude events ($M >= 5.0$) are explained by a stress tensor, which uses 94% of the data (16 over 17), with a pure strike-slip regime ($R' = 1.49 \pm 0.24$) and a NE-SW $S_{Hmax}$ (N146°E ± 7.5°). The two other classes give stress tensors, which represent only 63% and 69% of their representative data and markedly different $S_{Hmax}$ (N140°E ± 4.2° for $5.0 > M >= 4.5$ and N004°E ± 2.5° for $M < 4.5$). In the intraplate Saharan-Tunisian Atlas domain (Box 4), the stress inversion shows similar results for the entire data set and for the largest-magnitude subsets with a strike-slip regime ($R' = 1.65 \pm 0.12$) and a $S_{Hmax}$ (N165°E ± 6.9°). The smallest-magnitude mechanisms give a slightly more compressional regime (1.78 ± 0.17) and a similar $S_{Hmax}$ (N136°E ± 6.3°).

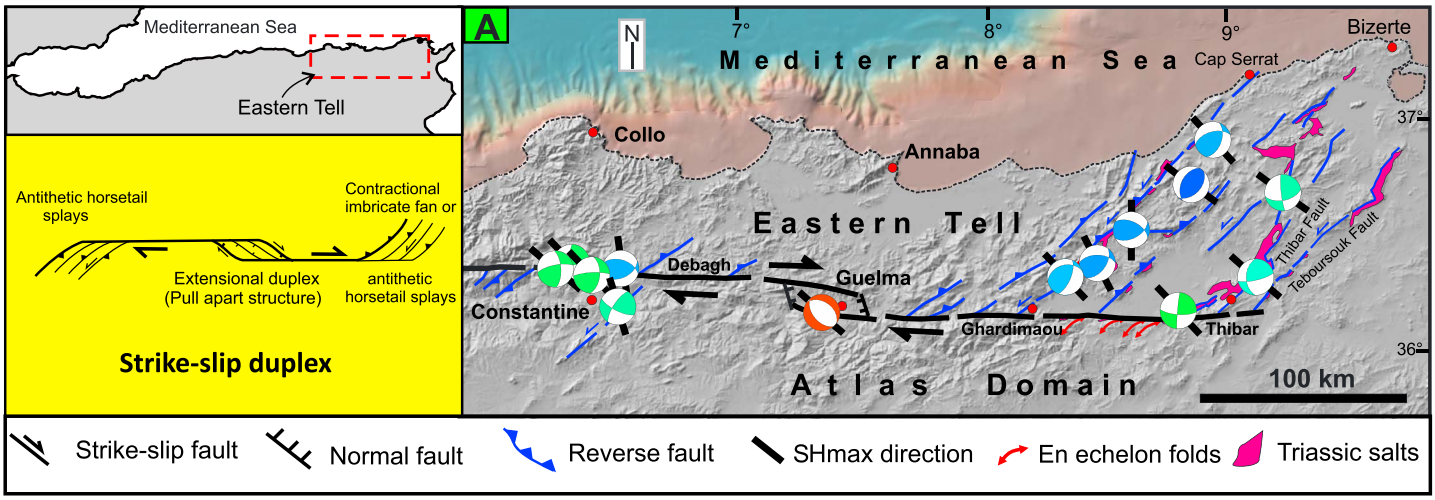


**Figure 3.** Active strike-slip fault system of Eastern Tell region. Focal mechanisms are from Heidbach et al. (2016) and Harvard CMT where the color is based on the triangle diagram in Figure 2.

Our results show that the studied convergent plate boundary (i.e., Maghreb region) is characterized by zones of less homogenous and more distributed tectonic deformation with a spatial variation of tectonic stress regime from east to west and north to south. Our stress field results are obtained by inversion of significant number of the largest-magnitude focal mechanism solutions representative of each major strike-slip fault zone of the Maghreb. They show a rather stable (within the error range) direction of $S_{Hmax}$ when considering inversion results from the largest-magnitude earthquakes. The Saharan-Tunisian Atlas (Box 4) displays a small anticlockwise rotation of $S_{Hmax}$ relative to the Eastern Tell (Box 1). Within the Alboran/Rif, the focal mechanisms are less homogeneous, with a variety of $S_{Hmax}$ orientations from NW-SE to N-S in function of the magnitude class but with a stable strike-slip stress regime. The stress regime changes laterally along the Maghreb coastal domains, strike slip with a slight extensional component in Eastern Tell ($R' = 1.35 \pm 0.23$), pure strike slip in the Alboran-Rif ($1.49 \pm 0.24$) but strike slip with thrust faulting in Western Tell ($R' = 2.43 \pm 0.21$). In the Saharan-Tunisian Atlas, it is again strike slip, but with a slight compressional component ($R' = 1.65 \pm 0.12$).

### 3.4. Smoothed Stress Trajectories

In order to analyze the regional pattern of the $S_{Hmax}$ orientation across the study area, we applied a stress smoothing method that provides mean $S_{Hmax}$ orientation and its variability on a regular grid (Müller et al., 1992; Rajabi et al., 2017; Ziegler & Heidbach, 2017). A detailed explanation of the stress smoothing method and its algorithm can be found in Ziegler and Heidbach (2017). We compiled 387 $S_{Hmax}$ data records (Figure 9) inferred from focal mechanism solutions, formal inversion of focal mechanism solutions, and neotectonic faults (i.e., Quaternary faults). In this study we used the smoothing algorithm developed by Müller et al. (1992) and Ziegler and Heidbach (2017) to calculate the mean and variability of the $S_{Hmax}$ orientation on a 0.25° grid. We used a quality and distance-based ranking of the data records. It means that A-quality data received a weight of 1, 0.75 for B-quality, 0.5 for C-quality, and 0.25 for D-quality. Furthermore, the closer a data record is to a grid point, the larger is its significance for the computed mean value. In order to compute the mean orientation of $S_{Hmax}$ at a grid point, at least three data records are required to be within the search radius ($<25°$) for the variability of the $S_{Hmax}$ orientation. Figure 9 illustrates the result of smoothing stress pattern based on our data incorporating the World Stress Map data.

## 4. Active Strike-Slip Fault Systems of the Maghreb

Across the North Africa, from Moroccan Rif-Alboran Sea at the West to Tunisia at the East, within the Maghrebides chain and Saharan-Tunisian Atlas (foreland), there are many natural examples of active complex strike-slip systems (Figures 3–6). The built of strike-slip shear zones along this region is best understood as a kinematic response to imposed boundary constraints (e.g., Billi et al., 2011; Meghraoui & Pondrelli, 2013; Serpelloni et al., 2007) of oblique active convergence between Eurasia and Africa. Hence, we selected the four

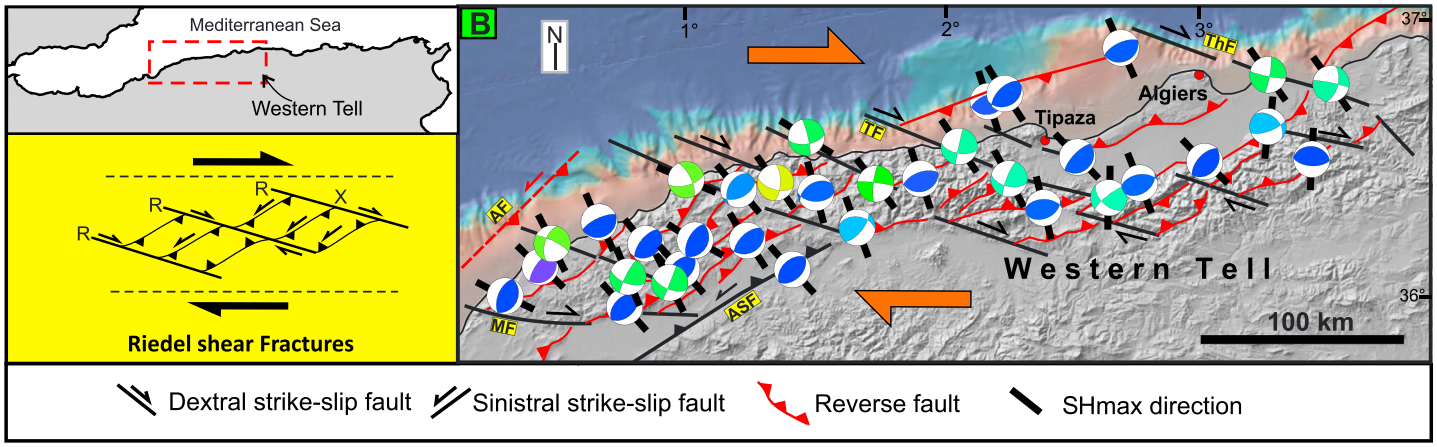


**Figure 4.** Active strike-slip fault system of the Western Tell region. Focal mechanisms are from Heidbach et al. (2016) and Harvard CMT where the color is based on the triangle diagram in Figure 2. AF: Arzew Fault; MF: Mostganem Fault; ASF: Asnam fault; TF: Tenès Fault; THF: Thenia Fault.

most significant examples of complex strike-slip faults distributed over the study region and show the seismotectonic activity and strain partitioning on these faulting systems. These examples will be described and analyzed in the following sections.

### 4.1. The Eastern Tell (Box 1)

The Eastern Tell belt, from Northeastern Algeria to Northern Tunisia, has been folded and faulted during the Alpine orogeny, with main paroxysmal NW-SE to NNW-SSE shortening phases during the Eocene, Miocene (e.g., Bracene & Frizon De Lamotte, 2002; Mattauer et al., 1977; Rouvier, 1977; Vila, 1980), and Quaternary (Ben Ayed, 1993; Harbi et al., 1999; Kherroubi et al., 2009; Meghraoui, 1988). Figure 3 summarizes the spatial distribution and tectonic style of the main faults identified in map views of the Eastern Tell region. It depicts one of a series of long, E-W right-lateral strike-slip crustal fault system (Aoudia et al., 2000; Jallouli et al., 2013) that is characteristic for northern Africa and extends over 200 km from the high mountains of Debagh (in Algeria; Meghraoui, 1988; Vila, 1980) in the west to Thibar region (in northern Tunisia) in the east. This E-W major fault zone is reported clearly in previous geological studies (e.g., Bounif et al., 1987; Guiraud, 1977; Maouche et al., 2013; Meghraoui, 1988; Rouvier, 1977; Vila, 1980), geophysical data (e.g., Amiri et al., 2011; Harbi et al., 1999) as a dextral strike-slip fault system. Moreover, it is characterized by neotectonic and seismotectonic activities (Harbi et al., 1999)

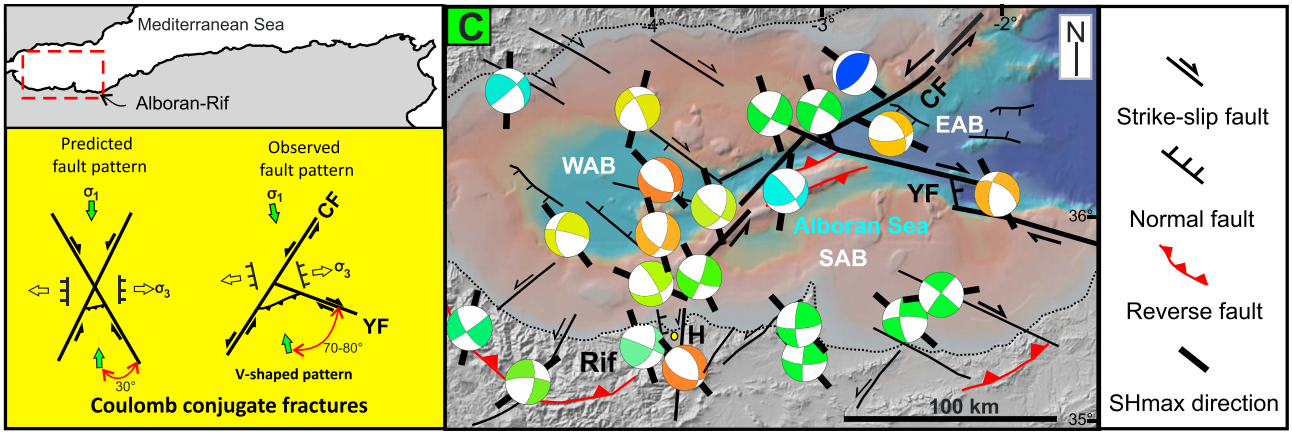


**Figure 5.** Map view of the active conjugate strike-slip fault system of the Alboran-Rif domain. CF: Carboneras fault system; YF: Yusuf fault; WAB: Western Alboran Basin; EAB: Eastern Alboran Basin; SAB: Southern Alboran Basin. Focal mechanisms are from Heidbach et al. (2016) and Harvard CMT where the color is based on the triangle diagram in Figure 2.

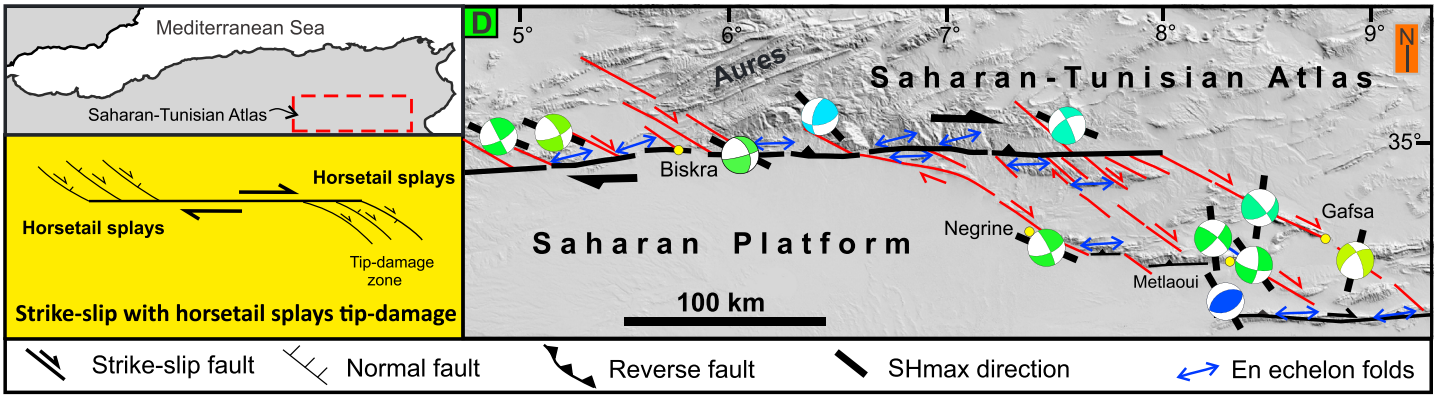


**Figure 6.** Map view of the intraplate active strike-slip fault of the Saharan-Tunisian Atlas. Focal mechanisms are from Heidbach et al. (2016) and Harvard CMT where the color is based on the triangle diagram in Figure 2.

and associated with en echelon folds along its westernmost fault segment and pull-apart basins along its easternmost segment (Maouche et al., 2013; Figure 3).

Several geological studies reveal the presence of magmatic rocks, diapiric Triassic salt outcrop (Maury et al., 2000; Rouvier, 1977; Vila, 1980), and hydrothermal activities (Maouche et al., 2013) along this major deep-seated fault system. The E-W trending master shear zone of Debagh-Thibar (DT) crossing the Guelma Basin (Harbi et al., 1999; Maouche et al., 2013; Meghraoui, 1988) combines and splays toward northern Tunisia with NE-SW trending features. These latter tectonic structures correspond to a complex assemblage of folds, thrusts, salt diapirs, oblique slip, and strike-slip faults (Figure 3), which were preferentially developed in the cover rocks with prevailing NE trending structural directions (e.g., Melki et al., 2012; Essid et al., 2016). Hence, the faulting architecture of this shear zone can be introduced as (1) an E-W trending postnappes (Neogene) and Quaternary strike-slip-pull-apart duplex of the Guelma Basin (Figure 3), formed between two major overlapping E-W dextral strike-slip segments of the DT, and (2) NE-SW contraction and imbricate faults or splays at the eastern tip in northwestern Tunisia. The contraction horsetail splays were expressed within the southeast verging Tellian nappes and Triassic diapiric zone. It is characterized by active NE-SW striking reverse faults with left-lateral slip originating in Pliocene and Quaternary such as the Ghardimaou-Cap Serrat and Teboursouk faults (Ben Ayed, 1993; Essid et al., 2016; Gueddiche et al., 1992; Rouvier, 1977; Soumaya et al., 2015). Along the two E-W fault segments limiting the pull-apart duplex of Guelma, several researchers have reported a neotectonic activity affecting the Quaternary deposits with mainly dextral strike-slip faulting (Bounif et al., 1987; Harbi et al., 1999; Maouche et al., 2013; Meghraoui, 1988; Vila, 1980).

The analysis of regional seismicity in the eastern Tell region, including focal mechanism solutions, shows a significant seismic activity along a band of less than 400-km width oriented mainly in the east-west direction (Harbi et al., 1999, 2003). Examples of important earthquakes within this region with significant surface ruptures are the $M_w$ 6.0 Constantine (27 October 1985), the $M_w$ 5.3 Laalam (20 March 2006), the $M_b$ 4.9 Kherrata (17 February 1949), the $M_s$ 5.2 Guelma (10 February 1937), and the $M_b$ 5.2 Thibar (20 February 1957) events (e.g., Beldjoudi et al., 2009; Bounif et al., 1987; Harbi et al., 2003; Ousadou et al., 2014; Soumaya et al., 2015). Most of these earthquakes are shallow and mainly accommodated through E-W and NE trending strike slip and NE reverse faulting (e.g., Aoudia et al., 2000; Harbi et al., 1999; Kherroubi et al., 2009). The NE and E-W fault directions correspond to the two nodal planes of the majority of focal mechanisms in this box (Figure 3). The two main E-W fault segments are dominated by right-lateral motions, while their eastern sections (anthetetic horsetail contraction splays) show the coexistence of left-lateral strike-slip and reverse faulting, which confirms the tectonic evidence. The normal seismic event in the Guelma zone (Aoudia et al., 2000) shows the reactivation of N-S to NNW-SSE bounding normal faults that constitutes the extensional duplex and intersects the subparallel main shear faults. Therefore, a local crustal extension (Maouche et al., 2013) occurs between two overlapping E-W dextral strike-slip faults under a regional-scale NW-SW compression. The stress tensor inversion of the largest-magnitude earthquakes ($M >= 4.5$) for the eastern Tell region (Figure 3) gives a strike-slip tectonic regime with a slight extensional component and NNW-SSE oriented $S_{Hmax}$ (N154°E ± 9.4°). In contrast, inversion of the small-magnitude events ($M < 4.5$) gives a thrust faulting

tectonic regime, slightly transpressional, with a NW-SE oriented $S_{Hmax}$ (N130°E ± 9.0°). This $S_{Hmax}$ orientation is consistent with the N134°E direction of global plate motion reported by DeMets et al. (1994).

The majority of focal mechanisms have E-W and NE-SW trending focal planes, suggesting a directional control by the reactivation of the main strike-slip system with their horsetail splays that form the dominant tectonic feature in this box. The major earthquake event that occurred in this area is the Constantine (1985, $M_w$ 6.0) seismic event and related NE strike-slip faulting (Bounif et al., 1987). The combination of a predominantly strike-slip faulting for the largest events ($R'$ = 1.35 ± 0.23) and reverse faulting for the smallest events ($R'$ = 2.24 ± 0.13) is expressed by an intermediate stress ratio of $R'$ = 1.61 ± 0.19 when inverting all focal mechanisms without distinction of magnitude class (Figure 7 and Table 1).

### 4.2. Western Tell (Box 2)

The recent and active tectonic deformations in the western continental part of the Tell are interpreted as transpressive faulting system, which results from the eastern continuation of the dextral motion along the Gloria transform fault and the Africa-Eurasia plate convergence (Meghraoui et al., 1996). The main tectonic features of this region (Figure 4) are (1) Mostganem fault, which may be the southeastern segment of NW-SE right-lateral Yusuf fault (Alvarez-Marrón, 1999; Meghraoui et al., 1996), (2) the Arzew Escarpment by a NE-SW left-lateral motion with reverse component, (3) the NE-SW trending El Asnam reverse fault with left-lateral component (Philip & Meghraoui, 1983), and (4) the NW-SE trending dextral strike-slip faults of Ténes and Thenia. Paleoseismological results (Holocene displacement) of the El Asnam fault show a Quaternary shortening rate of 0.4 mm to 0.6 mm/yr (Meghraoui, 1988), which imply a total shortening rate of ~2.2 mm/yr across the western Tell Atlas (Meghraoui & Doumaz, 1996). The observed seismicity is shallow, and the widespread earthquake distribution in the Western Tell (e.g., Ayadi et al., 2002) correlates well with the faults mapped in this region and provides evidence for ongoing reactivation of preexisting faults.

In this part of the Tell (Algeria), we suggest that active strike-slip fault systems deal sequentially with primary, synthetic and subsidiary antithetic systems of Riedel shear faults. The homogeneity of the Tell geology and tectonics during the Mesozoic and Cenozoic, and the strain-hardening deformation mechanism during Neogene and Quaternary (Bouhadad, 2001; Meghraoui et al., 1996), can favor the development of such highly systematic conjugate fault patterns with *R* and *X* fractures under the control of the E-W trending and right-lateral basement master shear faults. Here recent Paleomagnetic analysis along a narrow E-W major fault system pointed out that clockwise block rotation characterizes the active tectonics in the northern side of the Chelif basin (Aïfa et al., 1992; Derder et al., 2013). The ideal examples for the *R* fracture can be the Yusuf (SE segment), the Thenia, and the Ténes; the NE-SW trending Arzew left-lateral slip, Dahra, Boukadir, and El Asnam reverse faults (Meghraoui, 1988) may represent typical naturals examples of *X* conjugate fractures. From the late Miocene to present, the E-W trending crustal-scale right-lateral transcurrent faults seem to exert a major control on the conjugate Riedel fault system.

The seismicity distribution in the Central and Western Tell of Algeria is shallow and of widespread nature. It provides evidence of reactivation of preexisting faults and suggests its good correlation with geological features. This active deformation is mainly due to the NW to NNW oriented shortening generating purely compressive and strike-slip tectonic structures (Meghraoui et al., 1996; Ousadou et al., 2014, Figure 4). Several focal solutions of main shocks illuminate the existence of particular NW to E-W dextral strike-slip faulting. The NW oriented faults are suitable for *R* shears, while the NE-SW oriented faults would behave as *X*-conjugated shears along which occurs the significant stress release (Kariche et al., 2017). We also consider active as X-shears faults that were reactivated during the 1999 Ain Temouchent earthquake ($M_w$ 5.9) and the 1980 El Asnam earthquake ($M_w$ 7.3) as reverse faults with a left-lateral slip (Ayadi et al., 2002; Belabbes et al., 2008; Ousadou et al., 2014). This kinematic faulting associated with NW trending $S_{Hmax}$ favors the clockwise tectonic blocks rotation highlighted by Meghraoui and Pondrelli (2013) using structural and seismological data and confirmed using paleomagnetic data in the Chelif and Mitidja basins by Derder et al. (2013).

The stress inversion of the largest-magnitude focal mechanisms in this part of the Tell shows a compressive tectonic regime ($R'$ = 2.43 ± 0.21) with an NW-SE $S_{Hmax}$ (N147°E ± 9.4°) and a good (A) quality rank according to the World Stress Map quality ranking criteria (Table 1). The majority of the FMS have NW and NE trending focal planes (Figure 4), which suggests a directional control by the reactivation of NE-SW and NW-SE faults forming the main tectonic structures in this region. This result confirms that this segment of the plate

boundary is a transpressive deformed margin, where active NW trending dextral and NE reverse and sinistral faults are controlled by a first-order E-W right-lateral Riedel shear zone. In addition, we emphasize the key role of the master EW right-lateral transcurrent fault system of the Western Tell (Meghraoui et al., 1996) in the strain deformation and kinematic of synthetic (e.g., Tenès, Thenia and Yusuf faults as *R* fractures) and antithetic (e.g., El Asnam fault as *X* fracture) Riedel shears.

### 4.3. Rif-Alboran Block (Box 3)

The Rif-Alboran block constitutes a complex area of active deformation related to the oblique Africa-Eurasia convergence plates (e.g., Bousquet, 1979; Fadil et al., 2006; Martínez-García et al., 2011; Morel & Meghraoui, 1996; Palano et al., 2013; Soto et al., 2012; Figure 5). The most significant geological features of this region are represented by the curved structure of the Alboran Basin and the Rif chain including the Al-Hoceima seismic region and its surroundings (Figure 5). From the late Miocene to the present, the tectonic evolution of this area was controlled by major strike-slip faults (NW-SE right-lateral and NE-SW left-lateral faults) and governed by a NW-SE compression related to the plates convergence of Africa-Eurasia (e.g., Bezzeghoud & Buforn, 1999; Calais et al., 2003; Gracia et al., 2006; Martínez-García et al., 2011; Morel & Meghraoui, 1996; Serpelloni et al., 2007; Stich et al., 2003).

The Alboran Basin is crossed by the E-W to NW-SE trending right-lateral Yusuf fault from Gibraltar Straight to the Tell Atlas in Algeria. This major shear zone has a right-lateral transtensive fault kinematics, which includes the Yusuf pull-apart Basin (Meghraoui et al., 1996). The major fault separates the southern block with the Alboran ridge and Al Hoceima active zone, with the northern block and the offshore Betics structures and left-lateral NNE-SSW trending Carboneras fault (Bourgois et al., 1992; Gracia et al., 2006). With regard to the major Yusuf fault, the link of the adjoining shear zones shows two conjugate sets of Riedel shears: one has a NNE-SSW direction with left lateral shear sense and another with a SE orientation and right-lateral motion. Here the observed shear sense and fault orientations of the two major shear zones, present in the Alboran domain, can be suggested as a V-shaped conjugate strike-slip faults similar to that observed in western Turkey (Jackson & McKenzie, 1984; Şengör & Kidd, 1979). This mechanism could evolve into oblique strike-slip faults with obtuse angles in the compressive quadrant facing the $S_{Hmax}$ orientation (e.g., Cobbold & Davy, 1988; Jolivet et al., 1990; Tchalenko, 1970). In our case the V-shaped shear faults have an intersection with obtuse angle of 70–80° facing the NNW-SSE trending $S_{Hmax}$ (Figure 5), which is 30–45° larger than that predicted by the Anderson fault theory (Anderson, 1942). Therefore, we have an observed natural example of non-Andersonian conjugate strike-slip fault pattern.

The formation mechanism of V-shaped conjugate strike-slip faults is well developed in collisional orogens (Ratschbacher et al., 1991) and may have accommodated significant continental convergence (Sassier et al., 2009) such as our study case in the western Mediterranean (i.e., Alboran-Rif domain). V-shaped conjugate system includes Yusuf and Carboneras strike-slip faults (CF) that have been active since the Quaternary (Bousquet, 1979) with dextral and sinistral movements, respectively. North of the Yusuf lineament, the eastern subsiding Alboran Basin with Neogene age (depth $>$ 1,400 m), is located within the dilatational quadrant (eastern V-shaped) where it has been collapsed by reactivation of NE-SW grabens and normal faults trends (Ballesteros et al., 2008; Gutscher et al., 2002). However, the south Alboran Basin, with shallower basin floors ($<$ 1,200 m) (Martínez-García et al., 2011), forms the compressive quadrant (southern V-shaped) where it expands ENE-trending reverse faults and folds close the CF shear zone (Comas et al., 1999; Martínez-García et al., 2011; Willet, 1991), perpendicular to the $S_{Hmax}$ orientation (Figure 5).

Focal mechanism solutions in this block are mainly strike-slip faulting solutions with subordinately normal faulting toward the western and eastern Alboran Basins and few reverse mechanisms (Figure 7). The stress tensor computed on the largest-magnitude focal mechanisms ($M >= 5.0$; Box C, Figure 7) gives a clear strike-slip regime ($R' = 1.49 \pm 0.24$) and a NW oriented $S_{Hmax}$ (N146°E ± 7.5°; Table 1). It represents oblique strike-slip focal planes with sinistral NE-SW and dextral NW-SE planes. In the Western Alboran Basin and close to the Strait of Gibraltar, $S_{Hmax}$ orientation runs E-W and is related to a normal stress regime (Palano et al., 2013), which may be due to the active extensional forces exerted in the western dilatational quadrant of the Alboran V-Shaped conjugate strike-slip system. In its south compressive quadrant, there are subordinary reverse focal mechanism solutions (Figures 2 and 6), which may be due to the reactivation of thrust fault system under NNW-SSE stress regime. Along the southern CF fault segments, toward the Moroccan Rif, focal mechanism solutions show a primarily left-lateral strike-slip faulting stress regime (Figure 5). This NE-SW

trending fault system was active throughout the Neogene and Quaternary period, by contributing/reacting to the westward motion of the Gibraltar Arc (e.g., Bousquet, 1979; Masana et al., 2004). In the Al-Hoceima/Nekor region (southern limit of the CF shear zone), a band of strike-slip faults oriented roughly NE-SW, and associated with Neogene volcanism (Bousquet, 1979), is the site of shallow seismicity where the most important events are the 1994 and 2004 ($M_w$ 6.4) Al Hoceima earthquakes (e.g., Kariche et al., 2018; Medina, 1995; Ousadou et al., 2014; Stich et al., 2003). Oblique to the CF shear fracture, the current reactivation of the EW to SE trending conjugate Yusuf fault is marked by a right-lateral with normal component type of focal mechanism (Figure 5) in the vicinity of its pull-apart basin (Meghraoui et al., 1996).

GPS velocity data (Koulali et al., 2011) show an ~2–3 mm/yr NNE motion close to the Al-Hoceima region. The Rif Mountains, defining an E-W oriented fan-shaped feature, are moving WSW, and the Alboran ridge undergoes a clear NNW-SSE oriented contraction. Then, this region (part of a transpression system) is undergoing a coeval submeridian shortening, which is accommodated mainly by the active conjugate strike-slip faulting, associated with an east-west extension.

### 4.4. Saharan-Tunisian Atlas (Box 4)

The Atlas system of North Africa is located between the Tell/Rif belt to the north and the Saharan platform to the south (Figure 6). It is developed along crustal weakness zones inherited from Tethyan rifting episodes through basin inversions during Cenozoic to Quaternary, driven by the convergence of Africa toward Eurasia (Bracene & Frizon de Lamotte, 2002; Mattauer et al., 1977; Piqué et al., 2002). Along the eastern part of the SAF, between Algeria and Tunisia, the Cenozoic inversion gives a strong strike-slip component to the major south Atlasic basement fault (Arthaud & Matte, 1977; Ben Ayed, 1993; Swezey, 1996; Vially et al., 1994). Therefore, this intraplate shear zone may be initiated as major dip-slip discontinuities rift-bounding faults during the Mesozoic (Storti et al., 2003) that were subsequently reactivated. This major tectonic lineament considered as an intraplate right-lateral transpressive inversion structure (Addoum, 1995; Kazi-Tani, 1986; Panza et al., 2007) has several fault segments with different trends. In this study, we focus on the E-W strike-slip fault segment, crossing the Biskra region in eastern Algeria (Figure 6). At the fault segments eastern tip expands a succession of NW trending faults that we suggest as horsetail splay structures (e.g., Petit & Barquins, 1988), which branch at low angles from the master fault. Horsetail splay fractures tend to be developed where slip decreases out more gradually toward the fault tip (Brogi, 2011; Kim et al., 2000). Therefore, the master E-W strike-slip segment of Biskra shows NW-SE trending synthetic splay faults at its eastern tip or horsetail synthetic fractures subparallel to the local direction of maximum compressive stress (Soumaya et al., 2015) and accommodates the right-lateral slip. These structures include mainly the NW-SE trending dextral strike-slip of Gafsa, Metlaoui, and Negrine-Tozeur faults (Aissaoui, 1986; Ben Ayed, 1993; Boukadi et al., 1998; Zargouni et al., 1985). Westward and around the Biskra region, the main E-W fault trace is connected with NE-SW trending folds and by other NW trending horsetail splay faults with right-lateral motion (Figure 6). Furthermore, theses damage zones occur as result of stress concentrations, particularly at fault tips and intersection zones (e.g., Chester & Logan, 1986; Kim & Sanderson, 2006) or to accommodate displacement variations (Kim et al., 2000) along the Biskra major strike-slip fault (Addoum, 1995; Aissaoui, 1986).

The submeridian Quaternary shortening (e.g., Ben Ayed, 1993; Zargouni & Ruhland, 1981) was responsible for the reactivation with mainly strike-slip to transpressional regime (Aissaoui, 1986; Ben Ayed, 1993; Soumaya et al., 2015; Swezey, 1996; Vially et al., 1994; Zargouni & Ruhland, 1981) of the master Biskra fault (part of the SAF) and its associated eastern and western horsetail fractures. These splay structures are accompanied by NE to EW trending folds of Eocene to Quaternary age (Addoum, 1995; Aissaoui, 1986; Ben Ayed, 1993; El Ghali et al., 2003; Zargouni & Ruhland, 1981). Other studies (Frizon de Lamotte et al., 1998; Mercier et al., 1997) based on seismic profiles documented that the blind SAF, including the E-W Biskra fault, was reactivated locally as thrust/ramp fault during the Quaternary compression. The neotectonic reactivation (Quaternary compression phase) as dextral strike-slip fault of former E-W to NW-SE Mesozoic high-angle normal faults causes great structural complication with creation, in addition to conventional inversion, of ENE trending *en echelon* folds (Addoum, 1995) and faults that may be injected by Triassic salt (Letouzey et al., 1995; Vially et al., 1994). At the present day, the seismic activities with moderate to low magnitude ($M_w$ 3 to 5; Soumaya et al., 2015) is concentrated essentially at the SE termination of the main E-W strike slip (Figure 6). The most significant earthquakes events occurred mainly along the N120/N140°E deep strike

slip of Gafsa, Negrine, and Metlaoui faults (Soumaya et al., 2015) and subordinately across the NW trending en echelon faults around Biskra region (western horsetail splays). The repartition of focal mechanism solutions shows a prevailing strike-slip faulting regime on and around active NW-SE trending faults, such as Gafsa and Metlaoui faults, and a few reverse focal mechanism solutions along the E-W oriented faults (e.g., Northern Chott fault). The stress inversion result of the largest-magnitude focal mechanism solutions reveals a strike-slip tectonic regime with slight reverse component ($R' = 1.65 \pm 0.12$) and N148°E ± 6.9° $S_{Hmax}$ (Table 1). In fact, within this part of interplate shear zone (Booth-Rea et al., 2018), the seismic activities and focal mechanism solutions show a reactivation of the E-W deep-seated south Atlasic preexisting fault with strike-slip motion (in its eastern part) and its tip damage zones. This is in agreement with strike-slip to transpression-compatible paleostress results obtained for the neotectonic period (Soumaya et al., 2015; Vially et al., 1994).

## 5. Discussion

The data presented and analyzed in this paper show that major strike-slip fault systems and related structures characterize the Maghreb region tectonics. Indeed, E-W to NW-SE trending sheared zones played a key role in the accommodation and strain partitioning of the Neogene and active deformation. The geometries of these major strike-slip fault systems have been reviewed and newly described by four kinematic models. From this data set, it appears that strike-slip fault geometry (the distribution of discontinuities such as fault termination, and conjugate fractures) plays an important role in shaping the different Maghreb tectonic zones and controlling the active stress regime variations. Our findings point out that the primarily active contraction in the study area is partitioned and accommodated by the prevailing E-W dextral strike-slip duplex (in eastern Tell) with NE oriented contraction splays at its eastern edge, E-W dextral strike-slip fault with NW-SE horsetail splays (in the Saharan Atlas). Conjugate Riedel fault systems affect the western Tell with NE trending reverse thrust folds (*X* shears), WNW to NW directed dextral strike-slip faults (*R* shears). The Alboran-Rif block is expressed mainly by a V-shaped conjugate fault system with NE-SW left-lateral and E-W to NW-SE dextral strike-slip faulting.

### 5.1. Strike-Slip Faults and Active Tectonics

In the Rif-Alboran block, the active contraction found in our results is accommodated by the occurrence of primary strike-slip and subsidiary normal and reverse faulting earthquakes, which seem to be absorbed and partitioned mainly by major crustal/lithospheric tectonic structures of V-shaped conjugate shears of CF and Yusuf faults. Along and around these major fault traces there are predominant strike-slip events, while in the eastern and western V-shaped quadrants cohabit an extensional and strike-slip fault events. Near the intersections of theses major lineaments, some few reverse focal mechanisms (Figure 5) with left-lateral component are due perhaps to the reactivation of ENE-WSW thrust faults into southern V-shaped compressive quadrant. Furthermore, southwestward of the Yusuf shear zone and toward Gibraltar strait, Koulali et al. (2011) and Palano et al. (2013) reported an ~2.4 mm/yr of E-W crustal stretching and westward motion of the Alboran Basin accompanied by pull-apart normal faulting. While going away eastward of this active major shear fracture, the geodetic data show approximately NW strain-oriented axes, indicating a convergence rate of 2.5 to 5 mm/yr (Meghraoui & Pondrelli, 2013) across the plate boundary that is associated with a primarily thrust faulting regime along the western Algerian margins (Figure 4). Here we suggest that the CF and Alboran ridge act as barrier between two different active domains (eastern and western) with different motion and tectonic style.

The relative coincidence of this V-shaped conjugate fault system with the established plate boundary (Figures 7 and 10) allows us to propose the Yusuf fault as a broad lithospheric shear zone with right-lateral motion. This view is imposed by its reactivation as a primarily role in the prevailing transtensional tectonic regime into the Alboran/Rif block and western Mediterranean plate boundary zone. This is in agreement with the suggestion that major strike-slip faults can act as plate boundaries and be defined as narrow shear zones beneath the much thicker continental crust (e.g., Peltzer & Tapponnier, 1988; Tapponnier et al., 2001). Therefore, the crustal faults network of Alboran ridge, CF, and Yusuf can form a good example of V-shaped conjugate strike-slip systems developed in the western Mediterranean collisional orogen and separating two strong domains (i.e., Africa and Eurasia plates). A similar fault pattern with V-shaped conjugate fault system is documented in collisional settings such as central Tibet (e.g., England & Molnar, 1990; Yin & Taylor, 2011), western Turkey (Jackson & McKenzie, 1984; Şengör & Kidd, 1979), the eastern Alps (Ratschbacher et al., 1991), and central Mongolia (e.g., Calais et al., 2003; Cunningham, 2005).

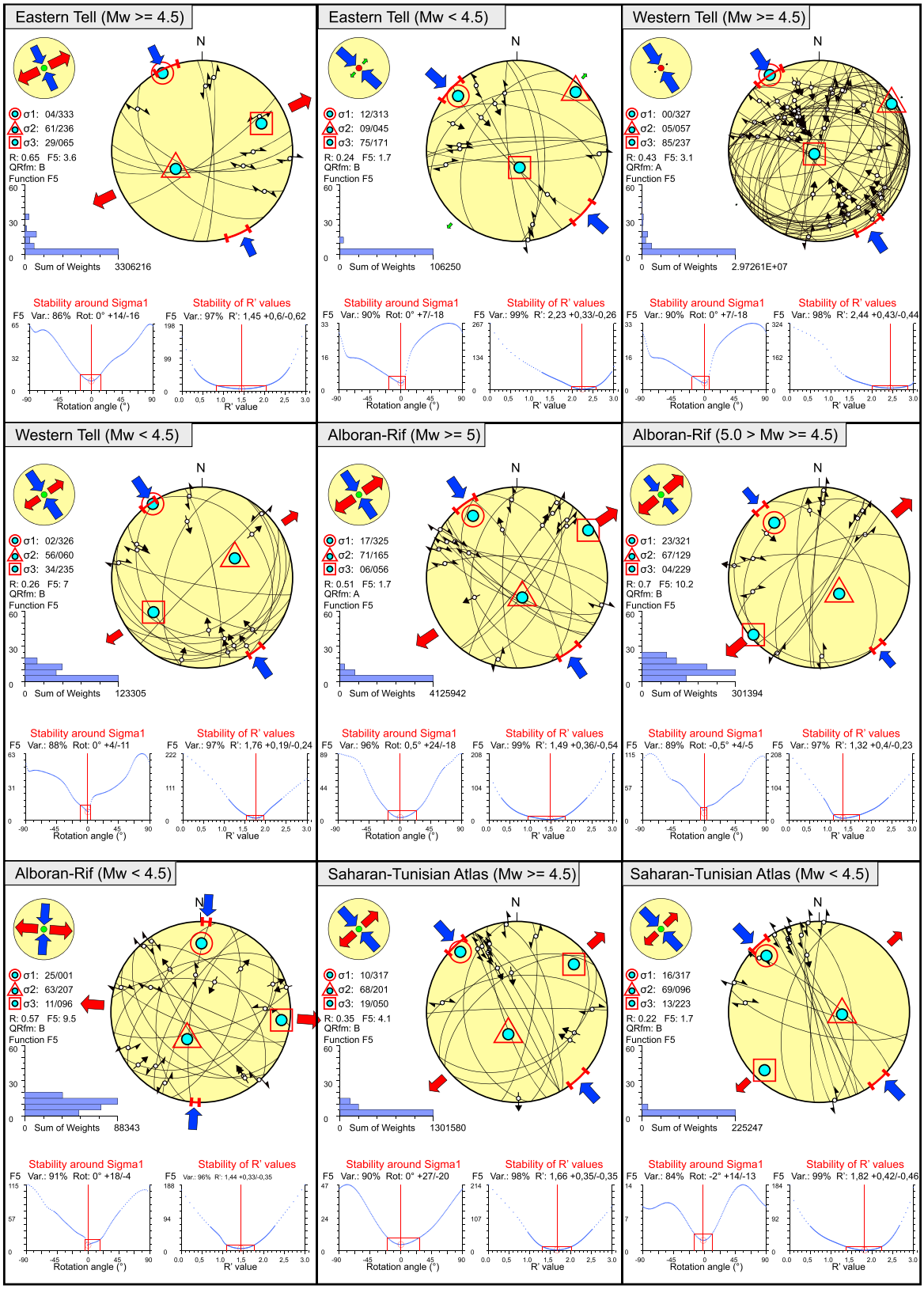


**Figure 7.** Stress inversion and focal plane selection results: lower hemisphere equal-area stereoplots of the selected focal planes with the three principal stress axes, horizontal stresses $S_{Hmax}$ and $S_{hmin}$. The histogram on the lower left corner of the figures represents the distribution of the misfit function F5. F5, misfit function and QRfm, Quality of the inferred $S_{Hmax}$ based on the World Stress Map ranking criteria.

In the Western Tell, active tectonics and earthquake fault plane solutions show dominant en echelon NE-SW trending thrust faults with high seismic magnitude (e.g., El Asnam, $M_w$ 7.3 1980) and subordinate NW to WNW trending dextral strike-slip events with relatively moderate to low magnitude (Meghraoui & Pondrelli, 2013). This reflects a prevailing current stress release along the NE-SW en echelon thrust-related folding structures and left-lateral strike-slip faults (as *X* conjugate fractures) more than on the NW-SE to WNW dextral strike-slip faults (as *R* fractures). This can explain the dominant current compressional stress regime with NW orientation found in this region (Figure 7). Furthermore, this cover faulting pattern with en echelon fractures, controlled by a major E-W right-lateral crustal tectonic structure, reinforces the model of clockwise small-block rotation with transpressional tectonic regime proposed by Meghraoui et al. (1996) confirmed by Derder et al. (2013) for this region and promotes more the NW oblique convergence of Africa-Eurasia plates.

Farther east, the major E-W trending right-lateral strike-slip fault system of DT, which terminates with numerous NE-SW thrusts and left-lateral horsetail faults (mainly in northern Tunisia) and forming a transtensional duplex within its central part (pull-apart basin of Guelma), accommodates the mainly active deformation in the eastern part of the Tell. These imbricate fault system, with several thrusts and left-lateral displacement, developed at a relative high-angle anticlockwise sense with E-W dextral master fault of DT. It has an antithetic faulting style perpendicularly with $S_{Hmax}$ orientation. The most important seismic energy release in this region is through strike-slip fault earthquakes such as $M_w$ 6.0, Constantine (1985), and $M_w$ 5.2, Thibar (1957). The normal faulting events of Guelma reveal the current oblique reactivation of the local releasing stepover (NNW-SSE) and pull-apart structure between the overlaps E-W fault segments of DT. Therefore, the reactivation of this master E-W crustal fault and its related faults implies the partitioning of the active deformation between mainly strike-slip, local normal faulting and subsidiary thrust faulting along the eastern Tell region. More generally, the formation of this E-W trending strike-slip duplex is best understood as a kinematic response to inherited geological structures and imposed boundary constraints as suggested by Woodcock and Fischer (1986), rather than by the stress control or bulk strain process ordinarily applied to wrench tectonics.

Along the Saharan-Tunisian Atlas, NW trending horsetail splay faults connect at a relative low-angle clockwise with the major right-lateral strike-slip fault of Biskra structural slip line. We note that theses subsidiary horsetail faults have a synthetic faulting style, similar to the right-lateral motion with the master fault and a subparallel orientation with $S_{Hmax}$. This is consistent with the model proposed by Kim and Sanderson (2006) for the variety of structures at the tips of strike-slip faults. Also, the main seismic release activity is concentrated along the NW-SE trending faults (eastern horsetail splays system), such as Gafsa, Metlaoui, and Negrine faults (Soumaya et al., 2015) with a dextral strike-slip stress regime (Figure 5). This aspect is in agreement with the model of Kim et al. (2000) and Kim and Sanderson (2006), which proposes that the displacement along the master fault decreases with time and finally dies out toward the strike-slip fault tip, transferring the majority of displacement onto splay faults. The neotectonic and current reactivation of this inherited deep fault system with strike-slip stress regime (e.g., Addoum, 1995; Soumaya et al., 2015; Vially et al., 1994) reinforces the idea that the intracontinental deformation within the crust and hence interplate seismicity is accommodated by reactivation of preexisting weakness zones, in particular strike-slip faults (Coward, 1994), and causes variations of local stress concentration (Campbell, 1978). Also, the active oblique deformation shown along this major intraplate South Atlas basement fault can support the suggestion of Molnar and Dayem, 2010) that the slip on many major intracontinental strike-slip faults absorbs large portions of relative plate motion between lithospheric plates (i.e., Africa-Eurasia) and deforming regions.

### 5.2. Spatial Pattern of $S_{Hmax}$ Orientation and Tectonic Regime Variations

Our results show a spatial distribution of orientation, kinematics, and active tectonic regime for the western Mediterranean Africa-Eurasia plate boundary. We evidence a change in the current tectonic regime from transpressional to compressional in the Tell and Atlas areas, to strike-slip/transtensional in the Alboran/Rif block, with a slight clockwise rotation of $S_{Hmax}$ orientations from the intraplate Saharan-Tunisian Atlas domain to the Tell domain. From east to west, the $S_{Hmax}$ orientations remain stable if we consider inversion results of the largest-magnitude earthquakes, but significant rotations are observed between the different magnitude class in the Alboran-Rif, with up to N-S orientation for the $M < 4.5$ solution. The inversion of

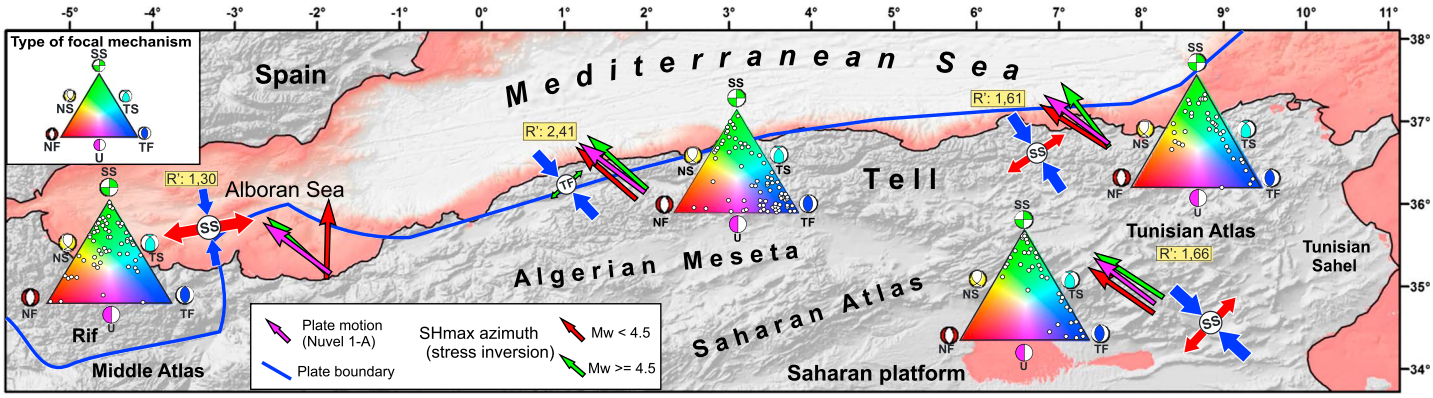


**Figure 8.** Stress pattern and tectonic regime variations along the Maghreb area. SS: strike-slip faulting; TF: thrust faulting regime.

stress tensor from FMS along the study region allows detecting a stress regime characterized by an always subhorizontal $\sigma 1$, with $\sigma 2$ and $\sigma 3$ close in magnitude (Figure 7a). Furthermore, the horizontal stresses become increasingly more compressive with respect to the vertical stress in the Western Tell (predominantly thrust mechanisms) relatively compared to Eastern Tell, and Saharan Atlas (characterized predominantly by strike-slip focal mechanisms). This discrepancy is expressed by stress axes permutation of $\sigma 2$ and $\sigma 3$ (Figure 7).

Due to lack of GPS data and strain rate field results for most parts of the Maghreb, we may compare the mean $S_{Hmax}$ orientation (N148°E ± 10.4°) based on the smoothed stress map (Figures 8–10) with relative and absolute plate motions inferred from NUVEL-1A geodetic model (DeMets et al., 1994), which are N134°E ± 15°. As demonstrated in Figures 10 and 11, the first-order $S_{Hmax}$ orientation in the Maghreb region is fairly consistent with relative plate motion of Africa with respect to the Eurasia and highlights the role of large tectonic forces in first-order stress pattern (Heidbach et al., 2016; Rajabi et al., 2017). In addition, there are numerous small $S_{Hmax}$ perturbations in the study area that reveal the role of other stress sources (i.e., mostly third order) that have been demonstrated as important sources in crustal deformation (Heidbach et al., 2016; Rajabi et al., 2016, 2017; Zoback, 1992).

Along the E-W trending Yusuf shear zone, stress indicators show an average submeridian $S_{Hmax}$ (Figure 9) with a significant clockwise rotation (>30°) relative to absolute plate motion associated by a southward motion (3 mm/yr) of the Rif Mountains relative to stable Africa (Fadil et al., 2006). However, westward near the Strait of Gibraltar, the current tectonic deformation (with 4.3 ± 0.5 mm/yr) occurs anticlockwise to $S_{Hmax}$ (N116°E) direction (McClusky et al., 2003) and is accompanied by a normal faulting regime (e.g., Billi et al., 2011; Serpelloni et al., 2007). The source of the local stress field deviation with counterclockwise rotation of $S_{Hmax}$ (~18°) with respect to the plate motion and extension tectonics west of Alboran Sea can be related to its crustal thickness and thick sedimentary depocenter shown by Platt et al. (2003) and Fernandez-Ibañez et al. (2007). Also, this tectonic depression can promote additional tensional stresses and gravitational potential energy for this region. Along the Alboran/Rif zone, $S_{Hmax}$ shows prevailing NNW orientations, which are relatively in agreement with results found by De Vicente et al. (2008) and Martínez-García et al. (2011) who documented a transtensive tectonic regime for this area, and with the average $S_{Hmax}$ orientation on the World Stress Map (Heidbach et al., 2016). In addition, the global $S_{Hmax}$ (N168°E ± 10.6°) orientation found by our analysis, not parallel to NUVEL-1A (4.5–5 mm/yr with 135°–120°) global plate motion model (DeMets et al., 1994), reinforces the moderate clockwise rotation (38°) around the Trans-Alboran (TA) shear zone revealed by Fernandez-Ibañez et al. (2007). Therefore, the dominant NE left-lateral shear deformation associated with an average NE-SW extension (Meghraoui & Pondrelli, 2013) and the westward motion evidenced by Palano et al. (2013) make the Alboran-Rif domain acting as a specific strike-slip to transtensional tectonic block between two convergent plates. Moreover, the conjugate shear zones of Alboran ridge-CF and Yusuf faults, expressing the plate boundary, with opposite shear sense, seem to add a more complexity and local deviations of the crustal stress field in the Alboran/Rif area.

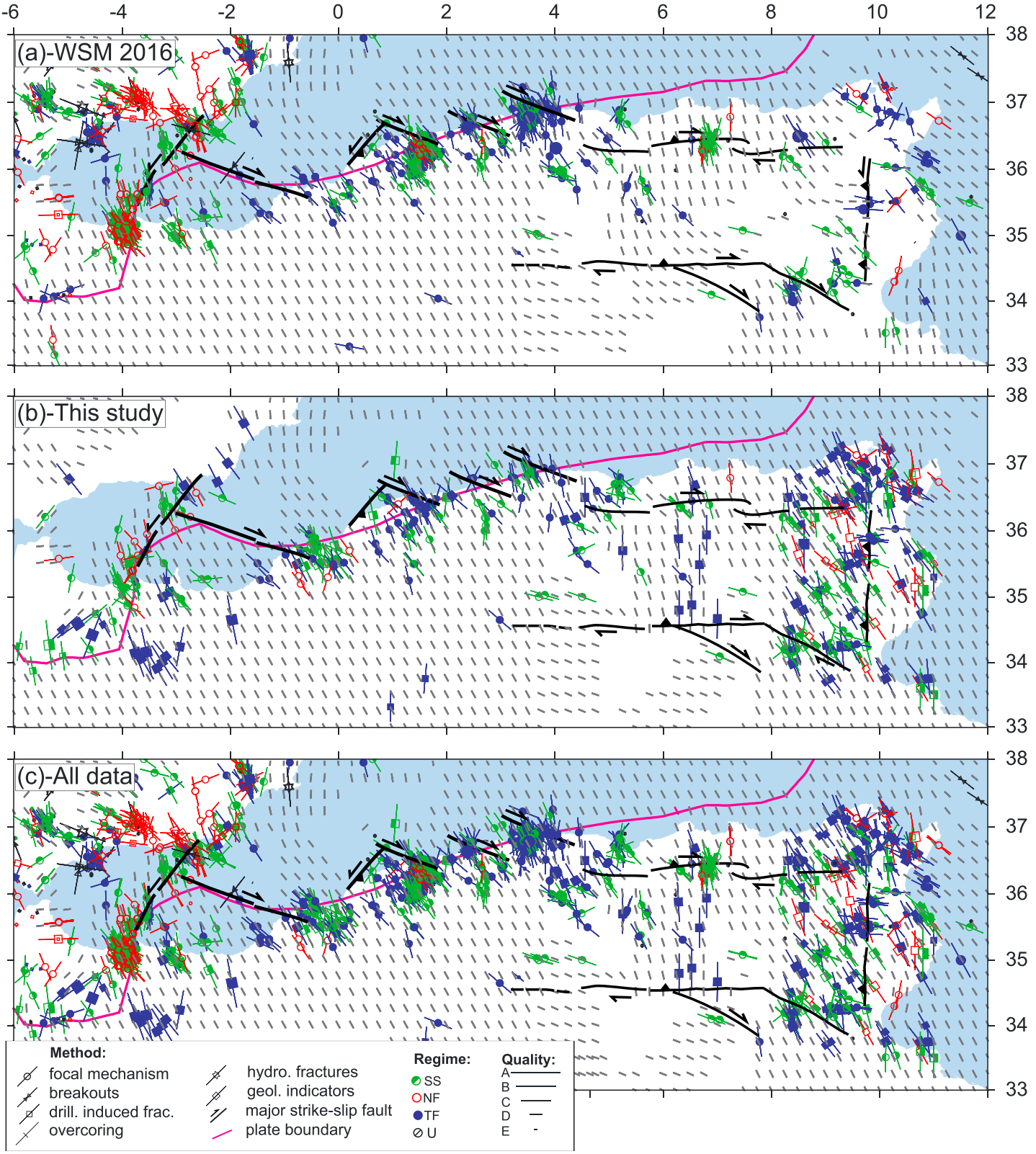


**Figure 9.** Stress map and smoothed stress pattern of the Maghreb region based on (a) the World Stress Map data and (b) our compilations. Different lines show the orientation of the $S_{Hmax}$ in which the length of the lines demonstrates the quality of the $S_{Hmax}$ orientations based on the World Stress Map ranking criteria: (a) the highest quality and (b) the lowest quality). Different colors show various tectonic stress regimes (red for normal, green for strike slip, and blue for thrust). Small gray lines are the results of smoothing stress algorithm that show the orientation of the $S_{Hmax}$ orientation across the region.

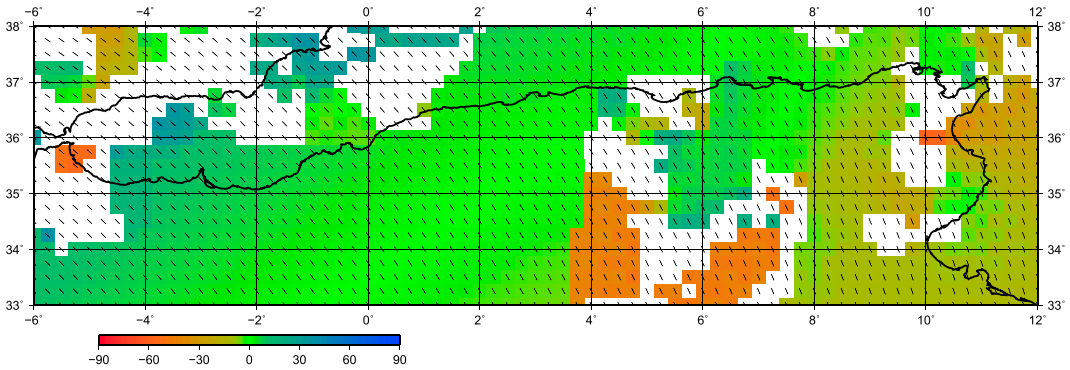


**Figure 10.** Comparison of the mean orientation of $S_{Hmax}$ and the direction of relative plate motion between the African and Eurasian plates according to DeMets et al. (1994), color coded on a 0.25° grid. In white areas no mean $S_{Hmax}$ data are available. The relative plate motion is indicated at each grid point by the black lines. Note that the color code indicates the angle of deviation between mean $S_{Hmax}$ and the direction of relative plat motion.

The N-S with clockwise rotation $S_{Hmax}$ deduced in the Eastern Tell using focal mechanisms is comparable to other major plate boundary strike-slip faults (i.e., the San Andreas Fault; Hickman et al., 2004; Townend & Zoback, 2004; Alpine fault of New Zealand; Rajabi, 2016; Townend et al., 2012; and Great Sumatran Fault; Mount & Suppe, 1992) because they may indicate weak fault physical properties (Hickman et al., 2004; Townend et al., 2012; Townend & Zoback 2004). In addition, strain directions of NUVEL-1A and $S_{Hmax}$ orientation (N145) revealed in eastern Tell by our stress inversion are quite similar, in contrast with the model of Ousadou et al. (2014), which predict N347° for $S_{Hmax}$, using the stress inversion of the single event of Constantine (1985). This discrepancy might be due to a transpression mechanism, by using mixed population of earthquake events (strike slip and reverse), with interactions between active thrusts a strike-slip faults across an over 300-km-long region. In addition, the WSW convergence directions considered by Sella et al. (2002), Calais et al. (2003), and Serpelloni et al. (2007) have a significant difference compared with NNW

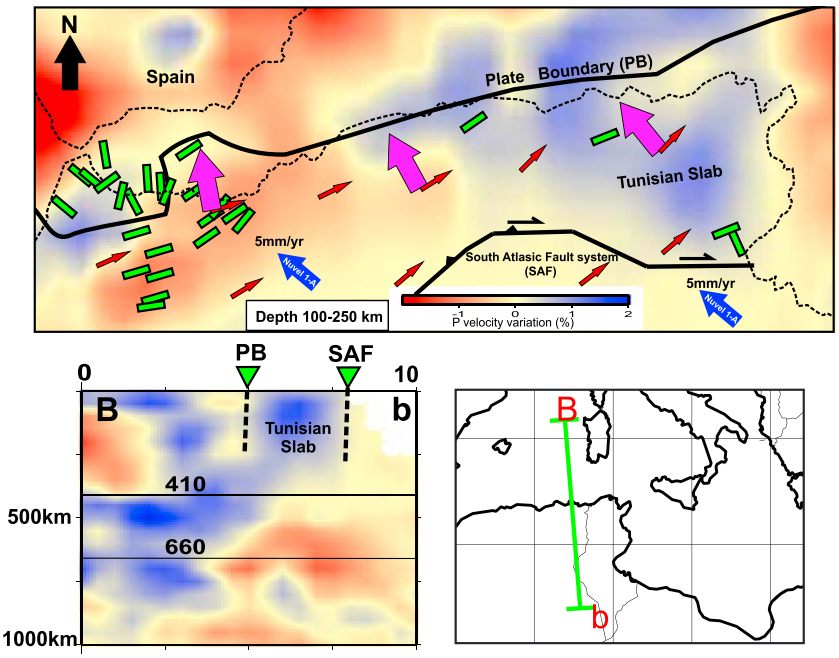


**Figure 11.** Reconstruction of the main geodynamic elements in the study region. Blue heavy line shows plate boundary (Bird, 2003); dark blue vector is the surface plate velocities from the NUVEL 1-A (DeMets et al., 1994); purple vectors show the $S_{Hmax}$ orientations; red vectors indicate the inferred motion of the mantle at 250-km depth (Faccenna et al., 2014); green sticks indicate SKS splitting measurements from the compilations of Faccenna et al. (2014) and references therein; the background is the tomography map from Piromallo and Morelli (2003).

trending $S_{Hmax}$ found in this paper. This is can due to the local perturbation induced by such strong seismic events as the 1994–2004 to 2016 in Al Hoceima or to the active conjugate strike-slip fault system of CF, Alboran ridge, and major Yusuf fault. In the Saharan-Tunisian Atlas, the stress trajectories of $S_{Hmax}$ are relatively consistent with the relative plate motion and accompanied by a significant third-order deviation in the vicinity of the deep-seated faults of Biskra and Tunisian North-South Axis (Figures 10 and 11). This local perturbation is manifested by an anticlockwise rotation of the $S_{Hmax}$ orientation that runs N-S and E-W, with a transpressive deformation regime, to a Biskra and the N-S Axis basement strike-slip faults, respectively (Figures 10 and 11).

At large scale, the interpreted present-day and neotectonic $S_{Hmax}$ runs NW-SE to NNW-SSE, interrupted by local perturbations, suggesting that plate-driving forces related to the Africa-Europe convergence impose the largest component of the total stress field. Furthermore, the coexistence of mixed focal mechanism solution (strike-slip and reverse events) into different Maghreb zones evidences further the suggested transpressive nature of the active Africa-Eurasia oblique convergence process (Meghraoui & Pondrelli, 2013). Westward of the study area (i.e., beyond Gibraltar and Atlantic domain) the African-Eurasian plate boundary segment along the Azores-Gloria region displays a mix of strike-slip and normal faulting seismic events, which grouped into an overall E-W trends (e.g., Custódio et al., 2016; Jiménez-Munt et al., 2010; Martínez-Loriente et al., 2013) with NW-SE trending $S_{Hmax}$ (Custódio et al., 2016). Eastward, the Africa-Europe contractional regime is mostly accommodated in the southern Tyrrhenian region with a NNW-SSE $S_{Hmax}$ by reactivation of an E-W trending thrust/backthrust systems (Billi et al., 2011; Pierdominici & Heidbach, 2012; Presti et al., 2013).

### 5.3. Driving Forces

In the lithosphere, stresses are caused by various sources that lead to the accumulation of strain energy mainly concentrated and released along the plate boundaries (Richardson et al., 1979). Most of previous studies reveal that the first-order stress field characterizing the North Africa (i.e., Maghreb region) is largely a consequence of compressional forces applied at a plate boundary, primarily ridge push and continental collision (e.g., DeMets et al., 1994; Meghraoui & Pondrelli, 2013; Nocquet, 2012; Serpelloni et al., 2007; Zoback, 1992). However, there are other forces of second and third order, which can generate additional stresses capable of influencing the active tectonic stress and faulting style shown in the Maghreb. Among them, we quote the residual stress accumulation that may be an additional force of second order in our study area, which increases in magnitude from one earthquake to the next, typically reaching failure level after several events and therefore reactivate a given inherited fault system (e.g., Lamarche & Tremblay, 2011; Saucier et al., 1992; Špičák, 1988). This kind of stress increases following a given major seismic event (e.g., Al Asnam) and can dominate the stress field near the fault (Špičák, 1988) with possibility of its migration from a segment fault to another. This is in agreement with the model of a stress transfer by the northeast trending earthquake migration along the Tell thrust-and-tear faults (Kariche et al., 2017; Lin et al., 2011). Another example of second-order sources of stress is the gravitational potential energy (Coblentz et al., 1998; Ghosh et al., 2009; Rajabi et al., 2017; Zoback, 1992), which characterizes the Alboran/Rif block (Palano et al., 2013). This gravitational field induced by lateral variations of crustal thickness and density could locally deviate the regional stress trajectories (Sonder, 1990) and change faulting style within the complex tectonic pattern of the Alboran Basin.

The Neogene collision-related compressional stresses (between Africa and Eurasia) can be transmitted far into forelands inducing the reactivation of preexisting crustal discontinuities such as the subvertical strike-slip fault system bounding at the South Saharan-Tunisian Atlas. These stresses were released along preexisting weak zones by seismic reactivation of ancient NW-SE and E-W dextral deep strike-slip faults of this region under a NW trending $S_{Hmax}$.

Among the processes that may adequately account for the vast majority of our surface and crustal deformation, we may quote the break off of subducting lithospheric slab and its lateral migration (e.g., Billi et al., 2011; Faccenna et al., 2004; Piromallo & Morelli, 2003), through the upper mantle flow pattern (e.g., Jolivet et al., 2009) and first-order preexisting weak zones (Wortel et al., 2009). Our stress inversion results reveal an average present-day NW trending transpression-compatible first-order stress regime that reactivated inherited structures (strike-slip/thrusts faults). These inherited fault systems, associated with basin inversions, are

mostly developed as a consequence of slab detachment, continental collision, and rollback toward the Calabrian and Gibraltar arcs (e.g., Faccenna et al., 2004). Furthermore, the spatial distribution of active deformation found at the tips of the Maghreb zone (i.e., Eastern Tell and Alboran) shows a clear tendency toward a strike-slip faulting stress regime, which could be linked to the mantle dynamics at the edges of this area, as suggested previously by Faccenna et al. (2014).

The SKS fast splitting directions (e.g., Civello & Margheriti, 2004; Faccenna et al., 2014) revealed that the upper mantle flow pattern, under the Maghrebides chain (eastern Tell) and its foreland (Saharan-Tunisian Atlas), is perpendicular to the *P* axis of focal mechanisms and the NW-SE $S_{Hmax}$ directions (Figure 11). This is consistent with the suggestion that mantle flow pattern generated by the eastward rollback motion of the Calabrian slab as reported by Piromallo and Morelli (2003) matches closely the present-day extensional orientation (Jolivet et al., 2009). Furthermore, the *T* axes trending of majorities of focal mechanisms characterizing the crustal earthquakes in the Saharan-Tunisian Atlas (Soumaya et al., 2015) is predominantly parallel to the plate boundary (Figures 2a and 7). This *T* axes uniformity can be interpreted as a reaction to the buoyancy forces of the lower crust caused by the rollback slab and by compressional stress transmitted within the foreland (i.e., Atlas domain) perpendicular to the Maghrebides collisional front. This suggested inference is in agreement with the interpretation of Singer et al. (2014) that viscous bending and stress transfer in the northern foreland of the Central Alps (related to the lateral extent of the European slab) is transformed to a compressional force in the foreland perpendicular to the Alpine front.

In the Rif-Alboran block, Fadil et al. (2006) suggested that the actual slab is probably the mantle part of the Alboran continental lithosphere, which has been detached from the crust and migrated to the south, due to the pull of an old slab. This motion pattern of the slab may be in favor of present-day surface/and crustal shearing with left-lateral component observed along the NE-SW CF and Alboran ridge fault systems. In addition, the upper mantle can also play an action on surface deformation, where the shear heating due to rise of magmas and/or hot fluids would inevitably cause strain localization in the deeper parts of strike-slip faults, as often shown in the field for crustal shear zones (Leloup et al., 1999). Therefore, we suggest a supplementary source of stress of mantle order that can accumulate along the crustal strike-slip faults of the Maghreb, such as the DT and Yusuf shear zones, which are associated by Neogene volcanism and hydrothermal activities (Bousquet, 1979; Maouche et al., 2013; Maury et al., 2000).

Based on tectonic reconstitutions, seismic tomography, geological, and geophysical evidence (Argnani, 2009; Booth-Rea et al., 2018; Govers & Wortel, 2005; Jolivet et al., 2009; Lucente & Margheriti, 2008; Wortel et al., 2009), we suggest a primary role of the first-order preexisting weak zones in the western Mediterranean, in particular the so-called Slab Transfer Edge Propagator (STEP) fault in the active geodynamics of the Maghreb. Near this E-W major transform fault system, along the Tell domain, there is a mix of reverse and strike-slip focal mechanism solutions (Figure 2a). The first-order transpressional regime that resulted for this region is in good agreement with the primary role expected by this STEP fault (Figure 11) with right-lateral kinematic. It created a free slab portion under the Eastern Tell and Saharan-Tunisian Atlas (Faccenna et al., 2004) where their southern edge is expressed at surface by the South Atlasic Fault system (Figure 11, cross sections B-b; Soumaya et al., 2015). Furthermore, the stress field rotation/deviation with E-W trends (Figure 9) has been explained by Soumaya et al. (2015) as a third-order stress perturbation along the STEP fault of the Tunisian N-S Axis. Hence, we predict that major preexisting structural tectonic weak zones and internal forces within the lithosphere and/or lithosphere-mantle interaction must contribute or even largely control the surface tectonic regime variation and stress field heterogeneities.

## 6. Conclusion

The stress field and active tectonic style within the Maghreb region are more heterogeneously distributed than commonly considered. Formal stress inversion of focal mechanism solutions shows a first-order transpression-compatible stress field and a second-order spatial variation of the present-day tectonic regime across the Maghreb region with clockwise rotation of $S_{Hmax}$ from east to west and a stress axes permutation. Therefore, the present-day active contraction of the western Africa-Eurasia boundary is accommodated by a strike-slip faulting regime with a normal component in the Alboran/Rif Block, a

predominantly NE-SW thrust faulting with a strike-slip component in the Western Tell part, and an E-W strike-slip faulting with reverse component along the Eastern Tell and Saharan-Tunisian Atlas. This spatial variation of the present-day stress field and faulting regime is in relative agreement with the stress field inferred from neotectonics features determined by others. The mean $S_{Hmax}$ direction displays a NW-SE orientation, suggesting that plate-driving forces, related to the Africa-Eurasia convergence, provide the major role on the regional stress pattern.

The geometries and roles of different major strike-slip fault systems in the Maghreb area has been reviewed and newly described. Exploring published results and proposed new kinematics models not proposed previously, we illustrate the role of the main geometrically complex shear zones of the Maghreb on the active stress field pattern. We suggest four models for the studied strike-slip fault systems: (1) a V-shaped conjugate fractures (TA and Yusuf shear zones), in the Alboran/Rif Block; (2) an E-W, right-lateral, Riedel transpressive shear zone within the western Tell area; (3) an E-W dextral strike-slip system with transtensional duplex in its central part and contractional splays at its eastern tip, in the Eastern Tell; and (4) an intraplate east trending, right-lateral, shear zone with horsetail splays in the Tunisia Sahara Atlas zone. These major inherited strike-slip faults and its related fractures accommodated the most oblique active convergence rate and impose their component on the second- and third-order stress regime throughout the Maghreb region, when reactivated.

In addition to first-order compressional forces applied at plate boundary (primarily ridge push and continental collision), which drives the regional stress field of the Maghreb, we suggest second and third order of stress sources as intersections of preexisting strike-slip faults, gravitational potential energy, and residual stresses for the Tell/Alboran/Rif belts and their Atlasic foreland (intracontinental). More generally, the current tectonic deformations and the upper crustal stress field in the Maghreb are governed by the interplay of the oblique plate convergence (i.e., Africa-Eurasia), lithosphere-mantle interaction, and preexisting weakness zones.

**Acknowledgments**
Moment tensors and focal mechanism solutions used in this work can be found free online at http://www.globalcmt.org; www.bo.ingv.it and http://www.world-stress-map.org/. The authors would like to thank John Geissman (Editor) and Laurent Jolivet (Associate Editor) for their advice and encouragements. We thank Claudia Piromallo, Assia Harbi and El Mabrouk Essid for their encouragement and helping. We also wish to thank Andrea Billi and Dominique Frizon de Lamotte for their constructive comments.

## References

Addoum, B. (1995). L'Atlas Saharien sud-oriental: Cinematique des plis-chevauchements et reconstitution du bassin du sud-est constantinois (confins algero-tunisiens), Paris 11.

Aïfa, T., Feinberg, H., Derder, M., & Merabet, N. (1992). Recent paleomagnetic rotations in the Cheliff basin (Algeria). *Comptes rendus de l'Académie des Sciences Série II*, *314*(9), 915–922.

Aissaoui (1986). Tectonique de l'Axe Biskra Negrine, Thèse de Doctorat en Science, Université de Strasbourg.

Alvarez-Marrón, J. (1999). Pliocene to Holocene structure of the eastern Alboran Sea (Western Mediterranean).

Alvarez, W., Cocozza, T., & Wezel, F. C. (1974). Fragmentation of the Alpine orogenic belt by microplate dispersal. *Nature*, *248*(5446), 309.

Amiri, A., Chaqui, A., Nasr, I. H., Inoubli, M. H., Ben Ayed, N., & Tlig, S. (2011). Role of preexisting faults in the geodynamic evolution of Northern Tunisia, insights from gravity data from the Medjerda valley. *Tectonophysics*, *506*(1–4), 1–10.

Anderson, E. M. (1942). The Dynamics of Faulting and Dyke Formation with Application to Britain (191 pp.). Edinburgh, Scotland: Oliver and Boyd.

Aoudia, A., Vaccari, F., Suhadolc, P., & Meghraoui, M. (2000). Seismogenic potential and earthquake hazard assessment in the Tell Atlas of Algeria. *Journal of Seismology*, *4*(1), 79–98. https://doi.org/10.1023/A:1009848714019

Argnani, A. (2009). Evolution of the southern Tyrrhenian slab tear and active tectonics along the western edge of the Tyrrhenian subducted slab. *Geological Society, London, Special Publications*, *311*(1), 193–212. https://doi.org/10.1144/SP311.7

Arthaud, F., & Matte, P. (1977). Late Paleozoic strike-slip faulting in southern Europe and northern Africa: Result of a right-lateral shear zone between the Appalachians and the Urals. *Geological Society of America Bulletin*, *88*(9), 1305–1320.

Auzende, J. M., Bonnin, J., & Olivet, J. L. (1973). The origin of the western Mediterranean basin. *Journal of the Geological Society*, *129*(6), 607–620. https://doi.org/10.1144/gsjgs.129.6.0607

Ayadi, A., Ousadou-Ayadi, F., Bourouis, S., & Benhallou, H. (2002). Seismotectonics and seismic quietness of the Oranie region (Western Algeria): The Mascara earthquake of August 18th 1994, $M_w$ = 5.7, $M_s$ = 6.0. *Journal of Seismology*, *6*(1), 13–23. https://doi.org/10.1023/A:1014276727136

Balanyá, J. C., Crespo-Blanc, A., Díaz Azpiroz, M., Expósito, I., & Luján, M. (2007). Structural trend line pattern and strain partitioning around the Gibraltar Arc accretionary wedge: Insights as to the mode of orogenic arc building. *Tectonics*, *26*, TC2005. https://doi.org/10.1029/2005TC001932

Ballesteros, M., Rivera, J., Muñoz, A., Muñoz-Martín, A., Acosta, J., Carbó, A., & Uchupi, E. (2008). Alboran Basin, southern Spain—Part II: Neogene tectonic implications for the orogenic float model. *Marine and Petroleum Geology*, *25*(1), 75–101.

Belabbes, S., Meghraoui, M., Cakir, Z., & Bouhadad, Y. (2008). InSAR analysis of ablind thrust rupture and related active folding: The 1999 Ain Temouchent earthquake ($M_w$ 5.7, Algeria) case study. *Journal of Seismology*, *13*(4), 421–432. https://doi.org/10.1007/s10950-008-9135-x

Beldjoudi, H., Guemache, M. A., Kherroubi, A., Semmane, F., Yelles-Chaouche, A. K., Djellit, H., et al. (2009). The Lâalam (Béjaïa, north-east Algeria) moderate earthquake (M w= 5.2) on March 20, 2006. *Pure and Applied Geophysics*, *166*(4), 623–640.

Ben Ayed, N. (1993). Evolution tectonique de l'avant-pays de la chaîne alpine de Tunisie du Début du Mésozoïque à l'Actuel. *Annales des Mines et de Géologie*, *32*, 286. https://tel.archives-ouvertes.fr/tel-01009784

Benaouali-Mebarek, N., Frizon de Lamotte, D., Roca, E., Barcène, R., Faure, R., Sassi, J.-L. W., & Roure, F. (2006). Post-Cretaceous kinematics of the atlas and tell systems in Central Algeria: Early foreland folding and subductionrelated deformation. *CR Geoscience, thematic issue: some recent developments on the geodynamics of the Maghreb*, *338*(1-2), 115–125. https://doi.org/10.1016/j.crte.2005.11.005

Bezzeghoud, M., & Buforn, E. (1999). Source parameters of the 1992 Melilla (Spain, $M_W$ = 4.8), 1994 Alhoceima (Morocco, $M_W$ = 5.8), and 1994 Mascara (Algeria, $M_W$ = 5.7) earthquakes and seismotectonic implications. *Bulletin of the Seismological Society of America*, *89*(2), 359–372.

Billi, A., Faccenna, C., Bellier, O., Minelli, L., Neri, G., Piromallo, C., et al. (2011). Recent tectonic reorganization of the Nubia-Eurasia convergent boundary heading for the closure of the western Mediterranean. *Bulletin de la Société Géologique de France*, *182*(4), 279–303.

Bird, P. (2003). An updated digital model of plate boundaries. *Geochemistry, Geophysics, Geosystems*, *4*(3), 1027. https://doi.org/10.1029/2001GC000252

Booth-Rea, S. G., Melki, F., Marzougui, W., Azañón, J. M., Zargouni, F., Galve, J., & Pérez-Peña, J. (2018). Late Miocene extensional collapse of Northern Tunisia. doi:https://doi.org/10.1029/2017TC004846

Bott, M. H. P. (1959). The mechanics of oblique slip faulting. *Geological Magazine*, *96*(02), 109–117.

Bouhadad, Y. (2001). The Murdjadjo, western Algeria, fault-related fold: Implications for seismic hazard. *Journal of Seismology*, *5*(4), 541–558. https://doi.org/10.1023/A:1012039900248

Bouillin, J. P. (1986). Le "bassin maghrébin": une ancienne limite entre l'Europe et l'Afrique à l'Ouest des Alpes. *Bulletin de la Societe Geologique de France*, *II*(4), 547–558.

Boukadi, N., Bédir, M., & Zargouni, F. (1998). Geometric and kinematic analyses of pullapart basins produced by en echelon strike-slip of Gafsa fault systems (Southern Tunisia). *Africa Geosciences Review*, *5*, 327–338.

Bounif, A., Haessler, H., & Meghraoui, M. (1987). The Constantine (northeast Algeria) earthquake of October 27, 1985: Surface ruptures and aftershock study. *Earth and Planetary Science Letters*, *85*(4), 451–460. https://doi.org/10.1016/0012-821X(87)90140-3

Bourgois, J., Mauffret, A., Ammar, A., & Demnati, A. (1992). Multichannel seismic data imaging of inversion tectonics of the Alboran Ridge (western Mediterranean Sea). *Geo-Marine Letters*, *12*(2-3), 117–122. https://doi.org/10.1007/BF02084921

Bousquet, J. C. (1979). Quaternary strike-slip faults in southeastern Spain. *Tectonophysics*, *52*(1-4), 277–286. https://doi.org/10.1016/0040-1951(79)90232-4

Bracene, R., & Frizon de Lamotte, D. (2002). The origin of intraplate deformation in the Atlas system of western and central Algeria: From Jurassic rifting to Cenozoic– Quaternary inversion. *Tectonophysics*, *257*.

Brogi, A. (2011). Variation in fracture patterns in damage zones related to strike-slip faults interfering with pre-existing fractures in sandstone (Calcione area, southern Tuscany, Italy). *Journal of Structural Geology*, *33*(4), 644–661. https://doi.org/10.1016/j.jsg.2010.12.008

Buforn, E., Bezzeghoud, M., Udias, A., & Pro, C. (2004). Seismic sources on the Iberia-African plate boundary and their tectonic implications. *Pure and Applied Geophysics*, *161*(3), 623–646. https://doi.org/10.1007/s00024-003-2466-1

Calais, E., DeMets, C., & Nocquet, J.-M. (2003). Evidence for a post-3.16-Ma change in Nubia–Eurasia–North America plate motions? *Earth and Planetary Science Letters*, *216*(1-2), 81–92. https://doi.org/10.1016/S0012-821X(03)00482-5

Campbell, D. L. (1978). Investigation of the stress-concentration mechanism for intraplate earthquakes. *Geophysical Research Letters*, *5*, 477–479. https://doi.org/10.1029/GL005i006p00477

Chalouan, A., Saji, R., Michard, A., & Bally, A. W. (1997). Neogene tectonic evolution of the southwestern Alboran Basin as inferred from seismic data off Morocco. *AAPG Bulletin*, *81*(7), 1161–1184.

Chester, F. M., & Logan, J. M. (1986). Implications for mechanical properties of brittle faults from observations of the Punchbowl fault zone, California. *Pure and Applied Geophysics*, *124*(1-2), 79–106.

Civello, S., & Margheriti, L. (2004). Toroidal mantle flow around the Calabrian slab (Italy) from SKS splitting. *Geophysical Research Letters*, *31*, L10601. https://doi.org/10.1029/2004GL019607

Cobbold, P., & Davy, P. (1988). Indentation tectonics in nature and experiment. 2: Central Asia. *Bulletin of the Geological Institution of the University of Upsala*, *14*, 143–162.

Coblentz, D. D., Zhou, S., Hillis, R. R., Richardson, R. M., & Sandiford, M. (1998). Topography, boundary forces, and the Indo-Australian intra-plate stress field. *Journal of Geophysical Research*, *103*, 919–931. https://doi.org/10.1029/97JB02381

Comas, M., García-Dueñas, V., & Jurado, M. (1992). Neogene tectonic evolution of the Alboran Sea from MCS data. *Geo-Marine Letters*, *12*(2-3), 157–164. https://doi.org/10.1007/BF02084927

Comas, M. C., Platt, J. P., Soto, J. I., & Watts, A. B. (1999). 44. The origin and tectonic history of the Alboran Basin: insights from Leg 161 results. In R. Zahn, M. C. Comas, & A. Klaus (Eds.), *Proceedings of the Ocean Drilling Program Scientific Results* (Vol. 161, pp. 555–580).

Coward, M. (1994). *Inversion tectonics, continental deformation* (pp. 289–304). Oxford: Pergamon.

Cunningham, D. (2005). Active intracontinental transpressional mountain building in the Mongolian Altai: Defining a new class of orogen. *Earth and Planetary Science Letters*, *240*(2), 436–444.

Custódio, S., Lima, V., Vales, D., Cesca, S., & Carrilho, F. (2016). Imaging active faulting in a region of distributed deformation from the joint clustering of focal mechanisms and hypocentres: Application to the Azores-western Mediterranean region. *Tectonophysics*, 676, 70–89.

Delvaux, D. (2012). Release of program Win-Tensor 4.0 for tectonic stress inversion: Statistical expression of stress parameters. EGU General Assembly, Vienna, 2012. *Geophysical Research Abstracts*, *14*, EGU2012–EGU5899.

Delvaux, D., & Barth, A. (2010). African stress pattern from formal inversion of focal mechanism data. *Tectonophysics*, *482*(1-4), 105–128. https://doi.org/10.1016/j.tecto.2009.05.009

Delvaux, D., Moeys, R., Stapel, G., Petit, C., Levi, K., Miroshnichenko, A., et al. (1997). Paleostress reconstructions and geodynamics of the Baikal region, Central Asia. Part II: Cenozoic rifting. *Tectonophysics*, *282*(1-4), 1–38. https://doi.org/10.1016/S0040-1951(97)00210-2

Delvaux, D., & Sperner, B. (2003). New aspects of tectonic stress inversion with reference to the TENSOR program. *Geological Society, London, Special Publications*, *212*(1), 75–100. https://doi.org/10.1144/GSL.SP.2003.212.01.06

DeMets, C., Gordon, R. G., Argus, D. F., & Stein, S. (1994). Effect of recent revisions to the geomagnetic reversal time scale on estimates of current plate motions. *Geophysical Research Letters*, *21*, 2191–2194. https://doi.org/10.1029/94GL02118

Derder, M. E. M., Henry, B., Maouche, S., Amenna, M., Bayou, B., Besse, J., et al. (2013). Transpressive tectonics along a major E-W crustal structure on the Algerian continental margin: Block rotation revealed by paleomagnetic investigations. *Tectonophysics*, *2013*(593), 183–192.

De Vicente, G. D., Cloetingh, S. A. P. L., Muñoz-Martín, A., Olaiz, A., Stich, D., Vegas, R. & Fernández-Lozano, J. (2008). Inversion of moment tensor focal mechanisms for active stresses around the microcontinent Iberia: Tectonic implications. *Tectonics*, *27*, TC1009. https://doi.org/10.1029/2006TC002093

Dewey, J., Helman, M., Knott, S., Turco, E., & Hutton, D. (1989). Kinematics of the western Mediterranean. *Geological Society, London, Special Publications*, *45*(1), 265–283. https://doi.org/10.1144/GSL.SP.1989.045.01.15

Domzig, A., Gaullier, V., Giresse, P., Pauc, H., Déverchère, J., & Yelles, K. (2009). Deposition processes from echo-character mapping along the western Algerian margin (Oran–Tenes), Western Mediterranean. *Marine and Petroleum Geology*, *26*(5), 673–694.

Durand-Delga, M., & Fontboté, J. M. (1980). Le cadre structural de la Méditerranée occidentale. Mémoire BRGM. 115 p.

El Ghali, A., Ben Ayed, N., Bobier, C., Zargouni, F., & Krima, A. (2003). Les manifestations tectoniques synsédimentaires associées à la compression éocène en Tunisie: implications paléogéographiques et structurales sur la marge Nord-Africaine. *Comptes Rendus Geoscience*, *335*(9), 763–771.

England, P., & Molnar, P. (1990). Right-lateral shear and rotation as the explanation for strike-slip faulting in eastern Tibet. *Nature*, *344*(6262), 140–142. https://doi.org/10.1038/344140a0

Essid, E. M., Kadri, A., Inoubli, M. H., & Zargouni, F. (2016). Identification of new NE-trending deep-seated faults and tectonic pattern updating in northern Tunisia (Mogodos–Bizerte region): Insights from field and seismic reflection data. *Tectonophysics*, *682*, 249–263. https://doi.org/10.1016/j.tecto.2016.05.032

Faccenna, C., Becker, T. W., Auer, L., Billi, A., Boschi, L., Brun, J. P., et al. (2014). Mantle dynamics in the Mediterranean. *Reviews of Geophysics*, *52*, 283–332. https://doi.org/10.1002/2013RG000444

Faccenna, C., Piromallo, C., Crespo-Blanc, A., Jolivet, L., & Rossetti, F. (2004). Lateral slab deformation and the origin of the western Mediterranean arcs. *Tectonics*, *23*, TC1012. https://doi.org/10.1029/2002TC001488

Fadil, A., Vernant, P., McClusky, S., Reilinger, R., Gomez, F., Sari, D. B., et al. (2006). Active tectonics of the western Mediterranean: Geodetic evidence for rollback of a delaminated subcontinental lithospheric slab beneath the Rif Mountains, Morocco. *Geology*, *34*(7), 529–532. https://doi.org/10.1130/G22291.1

Favre, P., & Stampfli, G. (1992). From rifting to passive margin: the examples of the Red Sea, Central Atlantic and Alpine Tethys. *Tectonophysics*, *215*(1-2), 69–97.

Fernandez-Ibañez, F., Soto, J., Zoback, M., & Morales, J. (2007). Present-day stress field in the Gibraltar Arc (western Mediterranean). *Journal of Geophysical Research*, *112*, B08404. https://doi.org/10.1029/2006JB004683

Frizon de Lamotte, D., Leturmy, P., Missenard, Y., Khomsi, S., Ruiz, G., Saddiqi, O., et al. (2009). Mesozoic and Cenozoic vertical movements in the atlas system (Algeria, Morocco, Tunisia): An overview. *Tectonophysics*, *475*(2009), 9–28.

Frizon de Lamotte, D., Mercier, E., Outtani, F., Addoum, B., Ghandriche, H., Ouali, J. B., & Andrieux, J. (1998). Structural inheritance and kinematics of folding and thrusting along the front of the eastern Atlas Mountains (Algeria and Tunisia). In S. Crasquin-Soleau & E. Barrier (Eds.), Péri-Tethys memoir 3 (1998). *Mémoires du Muséum d'histoire naturelle*, *177*, 237–252.

Frizon de Lamotte, D., Saint Bezar, B., Bracène, R., & Mercier, E. (2000). The two main steps of the Atlas building and geodynamics of the western Mediterranean. *Tectonics*, *19*, 740–761. https://doi.org/10.1029/2000TC900003

Frohlich, C. (1992). Triangle diagrams: Ternary graphs to display similarity and diversity of earthquake focal mechanisms. *Physics of the Earth and Planetary Interiors*, *75*(1–3), 193–198. https://doi.org/10.1016/0031-9201(92)90130-N

Gephart, J. W., & Forsyth, D. W. (1984). An improved method for determining the regional stress tensor using earthquake focal mechanism data: Application to the San Fernando earthquake sequence. *Journal of Geophysical Research*, *89*(B11), 9305–9320.

Ghosh, A., Holt, W. E., & Flesch, L. M. (2009). Contribution of gravitational potential energy differences to the global stress field. *Geophysical Journal International*, *179*(2), 787–812. https://doi.org/10.1111/j.1365-246X.2009.04326.x

Gomez, F., Beauchamp, W., & Barazangi, M. (2000). Role of the Atlas Mountains (northwest Africa) within the African-Eurasian plate-boundary zone. *Geology*, *28*(9), 775–778. https://doi.org/10.1130/0091-7613(2000)28<775:ROTAMN>2.0.CO;2

Govers, R., & Wortel, M. (2005). Lithosphere tearing at STEP faults: Response to edges of subduction zones. *Earth and Planetary Science Letters*, *236*(1-2), 505–523. https://doi.org/10.1016/j.epsl.2005.03.022

Gracia, E., Pallas, R., Soto, J. I., Comas, M., Moreno, X., Masana, E., et al. (2006). Active faulting offshore SE Spain (Alboran Sea): Implications for earthquake hazard assessment in the Southern Iberian Margin. *Earth and Planetary Science Letters*, *241*(3-4), 734–749. https://doi.org/10.1016/j.epsl.2005.11.009

Gueddiche, M., Harjono, H., Ben Ayed, N., & Hfaiedh, M. (1992). Analyse de la séismicité et mise en évidence d'accidents actifs. *Bulletin de la Société Géologique de France*, *163*(4), 415–425.

Guiraud, R. (1977). Sur la néotectonique des régions ouest-constantinoises. *Bulletin de la Société Géologique de France*, *7*(3), 645–650.

Gutscher, M. A., Malod, J., Rehault, J. P., Contrucci, I., Klingelhoefer, F., Mendes-Victor, L., & Spakman, W. (2002). Evidence for active subduction beneath Gibraltar. *Geology*, *30*(12), 1071–1074.

Harbi, A., Maouche, S., & Ayadi, A. (1999). Neotectonics and associate seismicity in the Eastern Tellian Atlas of Algeria. *Journal of Seismology*, *3*(1), 95–104. https://doi.org/10.1023/A:1009743404491

Harbi, A., Maouche, S., & Benhallou, H. (2003). Re-appraisal of seismicity and seismotectonics in the north-eastern Algeria Part II: 20 th century seismicity and seismotectonics analysis. *Journal of Seismology*, *7*(2), 221–234.

Heidbach, O., Rajabi, M., Reiter, K., Ziegler, M., & Team, W. S. M. (2016). World stress map database release 2016. *GFZ Data Services*. https://doi.org/10.5880/WSM.2016.001

Hickman, S., Zoback, M., & Ellsworth, W. (2004). Introduction to special section: preparing for the San Andreas Fault Observatory at Depth. *Geophysical Research Letters*, *31*, L12S01. https://doi.org/10.1029/2004GL020688

Jackson, J., & McKenzie, D. (1984). Active tectonics of the Alpine—Himalayan Belt between western Turkey and Pakistan. *Geophysical Journal International*, *77*(1), 185–264.

Jallouli, C., Mogren, S., Mickus, K., & Turki, M. M. (2013). Evidence for an east–west regional gravity trend in northern Tunisia: Insight into the structural evolution of northern Tunisian Atlas. *Tectonophysics*, *608*, 149–160. https://doi.org/10.1016/j.tecto.2013.10.003

Jiménez-Munt, I., Fernandez, M., Vergés, J., Afonso, J. C., Garcia-Castellanos, D., & Fullea, J. (2010). Lithospheric structure of the Gorringe Bank: Insights into its origin and tectonic evolution. *Tectonics*, *29*, TC5019. https://doi.org/10.1029/2009TC002458

Jolivet, L., Davy, P., & Cobbold, P. (1990). Right-lateral shear along the northwest Pacific margin and the India-Eurasia collision. *Tectonics*, *9*(6), 1409–1419.

Jolivet, L., & Faccenna, C. (2000). Mediterranean extension and the Africa-Eurasia collision. *Tectonics*, *19*, 1095–1106.

Jolivet, L., Faccenna, C., & Piromallo, C. (2009). From mantle to crust: Stretching the Mediterranean. *Earth and Planetary Science Letters*, *285*(1-2), 198–209. https://doi.org/10.1016/j.epsl.2009.06.017

Kariche, J., Meghraoui, M., Ayadi, A., & Boughacha, M. S. (2017). Stress change and fault interaction from a two century-long earthquake sequence in the central Tell Atlas (Algeria). *Bulletin of Seismological Society of America*, *107*(6), 2624–2635. https://doi.org/10.1785/0120170041

Kariche, J., Meghraoui, M., Timoulali, Y., Cetin, E., & Toussaint, R. (2018). The Al Hoceima earthquake sequence of 1994, 2004 and 2016: Stress transfer and poro-elasticity in the Rif and Alboran Sea region. *Geophysical Journal International*, *212*, 42–53. https://doi.org/10.1093/gji/ggx385

Kazi-Tani, N. (1986). Evolution géodynamique de la bordure nord africaine, le domaine intraplaque Nord Algérie. Approche mégaséquentielle. *Thesis ès-Sciences, Université de Pau et des Pays de l'Adour* (871 pp.).

Kherroubi, A., Déverchère, J., Yelles, A., De Lépinay, B. M., Domzig, A., Cattaneo, A., et al. (2009). Recent and active deformation pattern off the easternmost Algerian margin, Western Mediterranean Sea: New evidence for contractional tectonic reactivation. *Marine Geology*, *261*(1-4), 17–32. https://doi.org/10.1016/j.margeo.2008.05.016

Kim, Y.-S., Andrews, J. R., & Sanderson, D. J. (2000). Damage zones around strike-slip fault systems and strike-slip fault evolution, Crackington Haven, Southwest England. *Geosciences Journal*, *4*(2), 53–72. https://doi.org/10.1007/BF02910127

Kim, Y. S., & Sanderson, D. J. (2006). Structural similarity and variety at the tips in a wide range of strike–slip faults: A review. *Terra Nova*, *18*(5), 330–344. https://doi.org/10.1111/j.1365-3121.2006.00697.x

Koulali, A., Ouazar, D., Tahayt, A., King, R. W., Vernant, P., Reilinger, R. E., et al. (2011). New GPS constraints on active deformation along the Africa-Iberia plate boundary. *Earth and Planetary Science Letters*, *308*(1-2), 211–217. https://doi.org/10.1016/j.epsl.2011.05.048

Lamarche, C.-P., & Tremblay, R. (2011). Seismically induced cyclic buckling of steel columns including residual-stress and strain-rate effects. *Journal of Constructional Steel Research*, *67*(9), 1401–1410. https://doi.org/10.1016/j.jcsr.2010.10.008

Le Pichon, X., Bergerat, F., & Roulet, M.-J. (1988). Plate kinematics and tectonics leading to the Alpine belt formation: A new analysis. *Geological Society of America Special Papers*, *218*, 111–132. https://doi.org/10.1130/SPE218-p111

Leloup, P. H., Ricard, Y., Battaglia, J., & Lacassin, R. (1999). Shear heating in continental strike-slip shear zones: model and field examples. *Geophysical Journal International*, *136*(1), 19–40.

Leprêtre, R., Frizon de Lamotte, D., Combier, V., Gimeno-Vives, O., Mohn, G., & Eschard, R. (2018). The Tell-Rif orogenic system (Morocco, Algeria, Tunisia) and the structural heritage of the southern Tethys margin. *BSGF-Earth Sciences Bulletin*, *189*(2), 10. https://doi.org/10.1051/bsgf/2018009

Letouzey, J., Colletta, B., Vially, R., & Chermette, J. C. (1995). Evolution of salt-related structures in compressional settings. In M. P. A. Jackson, D. G. Roberts, & S. Snelson (Eds.), *Salt Tectonics: A Global Perspective: American Association of Petroleum Geologists (AAPG) Memoir* (Vol. 65, pp. 41–60).

Lin, J., Stein, R. S., Meghraoui, M., Toda, S., Ayadi, A., Dorbath, C., & Belabbes, S. (2011). Stress transfer among en echelon and opposing thrusts and tear faults: Triggering caused by the 2003 $M_w$ = 6.9 Zemmouri, Algeria, earthquake. *Journal of Geophysical Research*, *116*, B03305. https://doi.org/10.1029/2010JB007654

Lucente, F. P., & Margheriti, L. (2008). Subduction rollback, slab breakoff, and induced strain in the uppermost mantle beneath Italy. *Geology*, *36*(5), 375–378. https://doi.org/10.1130/G24529A.1

Lund, B., & Townend, J. (2007). Calculating horizontal stress orientations with full or partial knowledge of the tectonic stress tensor. *Geophysical Journal International*, *170*(3), 1328–1335. https://doi.org/10.1111/j.1365-246X.2007.03468.x

Maouche, S., Abtout, A., Merabet, N.-E., Aïfa, T., Lamali, A., Bouyahiaoui, B., et al. (2013). Tectonic and hydrothermal activities in Debagh, Guelma Basin (Algeria). *Journal of Geological Research*, *2013*, 1–13. https://doi.org/10.1155/2013/409475

Martínez-García, P., Soto, J. I., & Comas, M. (2011). Recent structures in the Alboran Ridge and Yusuf fault zones based on swath bathymetry and sub-bottom profiling: Evidence of active tectonics. *Geo-Marine Letters*, *31*(1), 19–36. https://doi.org/10.1007/s00367-010-0212-0

Martínez-Loriente, S., Gràcia, E., Bartolome, R., Sallarès, V., Connors, C., Perea, H., & Zitellini, N. (2013). Active deformation in old oceanic lithosphere and significance for earthquake hazard: Seismic imaging of the Coral Patch Ridge area and neighboring abyssal plains (SW Iberian Margin). *Geochemistry, Geophysics, Geosystems*, *14*(7), 2206–2231.

Masana, E., Martínez-Díaz, J. J., Hernández-Enrile, J. L., & Santanach, P. (2004). The Alhama de Murcia fault (SE Spain): A seismogenic fault in a diffuse plate boundary: Seismotectonic implications for the Ibero-Magrebian region. *Journal of Geophysical Research*, *109*, B01301. https://doi.org/10.1029/2002JB002359

Mattauer, M., Tapponnier, P., & Proust, F. (1977). Sur les mecanismes de formation des chaines intracontinentales: l9exemple des chaines atlasiques du Maroc. *Bulletin de la Société Géologique de France*, *7*(3), 521–526.

Mauffret, A. (2007). The northwestern (Maghreb) boundary of the Nubia (Africa) plate. *Tectonophysics*, *429*(1-2), 21–44. https://doi.org/10.1016/j.tecto.2006.09.007

Maury, R. C., Fourcade, S., Coulon, C., Bellon, H., Coutelle, A., Ouabadi, A., et al. (2000). Post-collisional Neogene magmatism of the Mediterranean Maghreb margin: A consequence of slab breakoff, Comptes Rendus de l'Académie des sciences-series IIA. *Earth and Planetary Science*, *331*(3), 159–173.

McClusky, S., Reilinger, R., Mahmoud, S., Ben Sari, D., & Tealeb, A. (2003). GPS constraints on Africa (Nubia) and Arabia plate motions. *Geophysical Journal International*, *155*(1), 126–138. https://doi.org/10.1046/j.1365-246X.2003.02023.x

McKenzie, D. P. (1969). The relation between fault plane solutions for earthquakes and the directions of the principal stresses. *Bulletin of the Seismological Society of America*, *59*(2), 591–601.

Medaouri, M., Déverchère, J., Graindorge, D., Bracene, R., Badji, R., Ouabadi, A., et al. (2014). The transition from Alboran to Algerian basins (western Mediterranean Sea): Chronostratigraphy, deep crustal structure and tectonic evolution at the rear of a narrow slab rollback system. *Journal of Geodynamics*, *77*, 186–205. https://doi.org/10.1016/j.jog.2014.01.003

Medina, F. (1995). Present-day state of stress in northern Morocco from focal mechanism analysis. *Journal of Structural Geology*, *17*(7), 1035–1046. https://doi.org/10.1016/0191-8141(94)00123-H

Meghraoui, M. (1988). Géologie des zones sismiques du Nord de l'Algérie: Paléosismologie, tectonique active et synthèse sismotectonique, (Doctorat d'Etat Thesis dissertation, 356 pp.). Paris 11-Orasy.

Meghraoui, M., Cisternas, A., & Philip, H. (1986). Seismotectonics of the Cheliff basin: Structural background of the El Asnam earthquake. *Tectonics*, *5*, 809–836. https://doi.org/10.1029/TC005i006p00809

Meghraoui, M., & Doumaz, F. (1996). Earthquake-induced flooding and paleoseismicity of the El Asnam (Algeria) fault-related fold. *Journal of Geophysical Research*, *101*, 17,617–17,644. https://doi.org/10.1029/96JB00650

Meghraoui, M., Morel, J.-L., Andrieux, J., & Dahmani, M. (1996). Tectonique plio-quaternaire de la chaine tello-rifaine et de la mer d'Alboran: Une zone complexe de convergence continent-continent. *Bulletin de la Société géologique de France*, *167*(1), 141–157.

Meghraoui, M., & Pondrelli, S. (2013). Active faulting and transpression tectonics along the plate boundary in North Africa. *Annals of Geophysics*, *55*(5). https://doi.org/10.4401/ag-4970

Melki, F., Zouaghi, T., Ben Chelbi, M., Bédir, M., & Zargouni, F. (2012). Role of the NE-SW Hercynian Master Fault Systems and Associated Lineaments on the Structuring and Evolution of the Mesozoic and Cenozoic Basins of the Alpine Margin, Northern Tunisia. In E. Sharkov (Ed.), *Tectonics-Recent Advances* (pp. 131–168). https://doi.org/10.5772/50145

Mercier, E., Outtani, F., & De Lamotte, D. F. (1997). Late-stage evolution of fault-propagation folds: principles and example. *Journal of Structural Geology*, *19*(2), 185–193.

Molnar, P., & Dayem, K. E. (2010). Major intracontinental strike-slip faults and contrasts in lithospheric strength. *Geosphere*, *6*(4), 444–467. https://doi.org/10.1130/GES00519.1

Morel, J. L., & Meghraoui, M. (1996). Goringe-Alboran-Tell tectonic zone: A transpression system along the Africa-Eurasia plate boundary. *Geology*, *24*(8), 755–758. https://doi.org/10.1130/0091-7613(1996)024<0755:GATTZA>2.3.CO;2

Mount, V. S., & Suppe, J. (1992). Present-day stress orientations adjacent to active strike-slip faults: California and Sumatra. *Journal of Geophysical Research*, *97*, 11,995–12,013. https://doi.org/10.1029/92JB00130

Müller, B., Zoback, M. L., Fuchs, K., Mastin, L., Gregersen, S., Pavoni, N., et al. (1992). Regional patterns of tectonic stress in Europe. *Journal of Geophysical Research*, *97*, 11,783–11,803. https://doi.org/10.1029/91JB01096

Negredo, A. M., Bird, P., Sanz de Galdeano, C., & Buforn, E. (2002). Neotectonic modeling of the Ibero-Maghrebian region. *Journal of Geophysical Research*, *107*(B11), 2292. https://doi.org/10.1029/2001JB000743

Nocquet, J. M. (2012). Present-day kinematics of the Mediterranean: A comprehensive overview of GPS results. *Tectonophysics*, *579*, 220–242. https://doi.org/10.1016/j.tecto.2012.03.037

Ousadou, F., Dorbath, L., Ayadi, A., Dorbath, C., & Gharbi, S. (2014). Stress field variations along the Maghreb region derived from inversion of major seismic crisis fault plane solutions. *Tectonophysics*, *632*, 261–280. https://doi.org/10.1016/j.tecto.2014.06.017

Palano, M., González, P. J., & Fernández, J. (2013). Strain and stress fields along the Gibraltar Orogenic Arc: Constraints on active geodynamics. *Gondwana Research*, *23*(3), 1071–1088. https://doi.org/10.1016/j.gr.2012.05.021

Panza, G. F., Raykova, R. B., Carminati, E., & Doglioni, C. (2007). Upper mantle flow in the western Mediterranean. *Earth and Planetary Science Letters*, *257*(1–2), 200–214. https://doi.org/10.1016/j.epsl.2007.02.032

Peltzer, G., & Tapponnier, P. (1988). Formation and evolution of strike-slip faults, rifts, and basins during the India-Asia collision: An experimental approach. *Journal of Geophysical Research*, *93*, 15,085–15,117. https://doi.org/10.1029/JB093iB12p15085

Petit, J. P., & Barquins, M. (1988). Can natural faults propagate under mode II conditions? *Tectonics*, *7*, 1243–1256. https://doi.org/10.1029/TC007i006p01243

Philip, H., & Meghraoui, M. (1983). Structural analysis and interpretation of the surface deformations of the El Asnam earthquake. *Tectonics*, *2*, 17–49. https://doi.org/10.1029/TC002i001p00017

Pierdominici, S., & Heidbach, O. (2012). Stress field of Italy—Mean stress orientation at different depths and wave-length of the stress pattern. *Tectonophysics*, *532*, 301–311.

Piqué, A., Tricart, P., Guiraud, R., Laville, E., Bouaziz, S., Amrhar, M., & Ouali, R. A. (2002). The Mesozoic-Cenozoic Atlas belt (North Africa): An overview. *Geodinamica Acta*, *15*(3), 185–208.

Piromallo, C., & Morelli, A. (2003). P wave tomography of the mantle under the Alpine-Mediterranean area. *Journal of Geophysical Research*, *108*(B2), 2065. https://doi.org/10.1029/2002JB001757

Platt, J., Whitehouse, M., Kelley, S., Carter, A., & Hollick, L. (2003). Simultaneous extensional exhumation across the Alboran Basin: Implications for the causes of late orogenic extension. *Geology*, *31*(3), 251–254. https://doi.org/10.1130/0091-7613(2003)031<0251:SEEATA>2.0.CO;2

Pondrelli, S., Salimbeni, S., Ekström, G., Morelli, A., Gasperini, P., & Vannucci, G. (2006). The Italian CMT dataset from 1977 to the present. *Physics of the Earth and Planetary Interiors*, *159*(3-4), 286–303. https://doi.org/10.1016/j.pepi.2006.07.008

Presti, D., Billi, A., Orecchio, B., Totaro, C., Faccenna, C., & Neri, G. (2013). Earthquake focal mechanisms, seismogenic stress, and seismotectonics of the Calabrian Arc, Italy. *Tectonophysics*, *602*, 153–175.

Rabaute, A, & Chamot-Rooke, N. (2014). Active tectonics of the Africa–Eurasia boundary from Algiers to Calabria (1/500 000). https://doi.org/10.13140/RG.2.2.23493.86245

Rajabi, M. (2016). Present-day crustal stress pattern across spatial scales: Analysis and interpretation from plate-wide to local-scales, (PhD thesis, 341 pp.). University of Adelaide, Adelaide.

Rajabi, M., Tingay, M., & Heidbach, O. (2016). The present-day stress field of New South Wales, Australia. *Australian Journal of Earth Sciences*, *63*(1), 1–21. https://doi.org/10.1080/08120099.2016.1135821

Rajabi, M., Tingay, M., Heidbach, O., Hillis, R., & Reynolds, S. (2017). The present-day stress field of Australia. *Earth-Science Reviews*, *168*, 165–189. https://doi.org/10.1016/j.earscirev.2017.04.003

Ratschbacher, L., Frisch, W., Linzer, H. G., & Merle, O. (1991). Lateral extrusion in the eastern Alps. Part 2: Structural analysis. *Tectonics*, *10*, 257–271. https://doi.org/10.1029/90TC02623

Rebaï, S., Philip, H., & Taboada, A. (1992). Modern tectonic stress field in the Mediterranean region: Evidence for variation in stress directions at different scales. *Geophysical Journal International*, *110*(1), 106–140. https://doi.org/10.1111/j.1365-246X.1992.tb00717.x

Richardson, R. M., Solomon, S. C., & Sleep, N. H. (1979). Tectonic stress in the plates. *Reviews of Geophysics*, *17*, 981–1019. https://doi.org/10.1029/RG017i005p00981

Roure, F., Casero, P., & Addoum, B. (2012). Alpine inversion of the North African margin and delamination of its continental lithosphere. *Tectonics*, *31*, TC3006. https://doi.org/10.1029/2011TC002989

Rouvier, H. (1977). Géologie de l'extrême nord tunisien: Tectoniques et paléogéographies superposés à l'extrémité de la chaîne nord maghrébine, Univ. P. and M. Curie (703p.).

Royden, L. H. (1993). Evolution of retreating subduction boundaries formed during continental collision. *Tectonics*, *12*, 629–638. https://doi.org/10.1029/92TC02641

Sassier, C., Leloup, P.-H., Rubatto, D., Galland, O., Yue, Y., & Lin, D. (2009). Direct measurement of strain rates in ductileshear zones: A new method based on syntectonic dikes. *Journal of Geophysical Research*, *114*, B01406. https://doi.org/10.1029/2008JB005597

Saucier, F., Humphreys, E., & Weldon, R. (1992). Stress near geometrically complex strike-slip faults: Application to the San Andreas Fault at Cajon Pass, Southern California. *Journal of Geophysical Research*, *97*, 5081–5094. https://doi.org/10.1029/91JB02644

Sella, G. F., Dixon, T. H., & Mao, A. (2002). REVEL: A model for recent plate velocities from space geodesy. *Journal of Geophysical Research*, *107*(B4), 2081. https://doi.org/10.1029/2000JB000033

Şengör, A. M. C., & Kidd, W. S. F. (1979). Post-collisional tectonics of the Turkish-Iranian plateau and a comparison with Tibet. *Tectonophysics*, *55*(3-4), 361–376.

Serpelloni, E., Vannucci, G., Pondrelli, S., Argnani, A., Casula, G., Anzidei, M., et al. (2007). Kinematics of the Western Africa-Eurasia plate boundary from focal mechanisms and GPS data. *Geophysical Journal International*, *169*(3), 1180–1200.

Singer, J., Diehl, T., Husen, S., Kissling, E., & Duretz, T. (2014). Alpine lithosphere slab rollback causing lower crustal seismicity in northern foreland. *Earth and Planetary Science Letters*, *397*, 42–56. https://doi.org/10.1016/j.epsl.2014.04.002

Sonder, L. J. (1990). Effects of density contrasts on the orientation of stresses in the lithosphere: Relation to principal stress directions in the Transverse Ranges, California. *Tectonics*, *9*, 761–771. https://doi.org/10.1029/TC009i004p00761

Soto, J. I., Fernández-Ibáñez, F., & Talukder, A. R. (2012). Recent shale tectonics and basin evolution of the NW Alboran Sea. *The Leading Edge*, *31*(7), 768–775. https://doi.org/10.1190/tle31070768.1

Soumaya, A., Ben Ayed, N., Delvaux, D., & Ghanmi, M. (2015). Spatial variation of present-day stress field and tectonic regime in Tunisia and surroundings from formal inversion of focal mechanisms: Geodynamic implications for central Mediterranean. *Tectonics*, *34*, 1154–1180. https://doi.org/10.1002/2015TC003895

Soumaya, A., Ben Ayed, N., Khayati Ammar, H., Kadri, A., Zargouni, F., Ghanmi, M. & Hfaiedh, M. (2016). Seismotectonic and seismic hazard map of Tunisia. CCGM, first edition.

Špičák, A. (1988). Interpretation of tectonic stress orientation on the basis of laboratory model experiments. *Physics of the Earth and Planetary Interiors*, *51*(1-3), 101–106. https://doi.org/10.1016/0031-9201(88)90028-3

Stich, D., Ammon, C. J., & Morales, J. (2003). Moment tensor solutions for small and moderate earthquakes in the Ibero-Maghreb region. *Journal of Geophysical Research*, *108*(B3), 2148. https://doi.org/10.1029/2002JB002057

Storti, F., Holdsworth, R. E., & Salvini, F. (2003). Intraplate strike-slip deformation belts. *Geological Society, London, Special Publications*, *210*(1), 1–14.

Swezey, C. (1996). Structural controls on Quaternary depocentres within the Chotts Trough region of southern Tunisia. *Journal of African Earth Sciences*, *22*(3), 335–347. https://doi.org/10.1016/0899-5362(96)00012-7

Tapponnier, P., Zhiqin, X., Roger, F., Meyer, B., Arnaud, N., Wittlinger, G., & Jingsui, Y. (2001). Oblique stepwise rise and growth of the Tibet Plateau. *Science*, *294*(5547), 1671–1677.

Tchalenko, J. (1970). Similarities between shear zones of different magnitudes. *Geological Society of America Bulletin*, *81*(6), 1625–1640. https://doi.org/10.1130/0016-7606(1970)81[1625:SBSZOD]2.0.CO;2

Townend, J., & Zoback, M. D. (2004). Regional tectonic stress near the San Andreas fault in central and southern California. *Geophysical Research Letters*, *31*, L15S11. https://doi.org/10.1029/2003GL018918

Townend, J., Sherburn, S., Arnold, R., Boese, C., & Woods, L. (2012). Three-dimensional variations in present-day tectonic stress along the Australia–Pacific plate boundary in New Zealand. *Earth and Planetary Science Letters*, *353*, 47–59.

Vially, R., J. Letouzey, F. Benard, N. Haddadi, G. Desforges, H. Askri, & A. Boudjema (1994). Basin inversion along the North African Margin. The Saharan Atlas (Algeria), Peri-tethyan platforms, 79–118.

Vila, J.-M. (1980). La chaîne alpine d'Algérie orientale et des confins algéro-tunisiens.

Wildi, W. (1983). La chaîne tello-rifaine (Algérie, Maroc, Tunisie): Structure, stratigraphie et évolution du Trias au Miocène. *Revue de Geographie Physique et de Geologie Dynamique*, *24*(3), 201–297.

Willet, A. (1991). Marine geophysical investigations of the Alboran Sea, (Unpublished PhD thesis). University of Oxford, Oxford.

Woodcock, N. H., & Fischer, M. (1986). Strike-slip duplexes. *Journal of Structural Geology*, *8*(7), 725–735.

Wortel, M., & Spakman, W. (2000). Subduction and slab detachment in the Mediterranean-Carpathian region. *Science*, *290*(5498), 1910–1917. https://doi.org/10.1126/science.290.5498.1910

Wortel, R., Govers, R., & Spakman, W. (2009). Continental collision and the STEP-wise evolution of convergent plate boundaries: From structure to dynamics. *Subduction Zone Geodynamics*, 47–59. https://doi.org/10.1007/978-3-540-87974-9_3

Yelles, A., Domzig, A., Déverchère, J., Bracène, R., Mercier, B., & Lépinay, D. (2009). Tectonophysics Plio-Quaternary reactivation of the Neogene margin off NW Algiers, Algeria: The Khayr al Din bank. *Tectonophysics*, *475*(1), 98–116. https://doi.org/10.1016/j.tecto.2008.11.030

Yielding, G., Ouyed, M., King, G., & Hatzfeld, D. (1989). Active tectonics of the Algerian Atlas Mountains-evidence from aftershocks of the 1980 El Asnam earthquake. *Geophysical Journal International*, *99*(3), 761–788. https://doi.org/10.1111/j.1365-246X.1989.tb02057.x

Yin, A., & Taylor, M. H. (2011). Mechanics of V-shaped conjugate strike-slip faults and the corresponding continuum mode of continental deformation. *Geological Society of America Bulletin*, *123*(9–10), 1798–1821. https://doi.org/10.1130/B30159.1

Zargouni, F., Rabia, M. C., & Abbes, C. (1985). Rôle des couloirs de cisaillement de Gafsa et de Negrine-Tozeur dans la structuration du faisceau des plis des Chott, éléments de l'accident sud-atlasique, Comptes rendus de l'Académie des sciences. Série 2, Mécanique, Physique, Chimie, Sciences de l'Univers. *Sciences de la Terre*, *301*(11), 831–834.

Zargouni, F., & Ruhland, M. (1981). Style de déformation du Quaternaire récent lié au coulissement de la faille de Gafsa et chronologie des phases tectoniques de l'Atlas méridional tunisien. *CR Acad. Sci. Paris*, *292*, 912–915.

Ziegler, M. O., & Heidbach, O. (2017). Manual of the Matlab Script Stress2Grid. World Stress Map Technical Report 17-02, GFZ German Research Centre for Geosciences. https://doi.org/10.2312/wsm.2017.002

Zoback, M. L. (1992). First-and second-order patterns of stress in the lithosphere: The World Stress Map project. *Journal of Geophysical Research*, *97*, 11,703–11,728. https://doi.org/10.1029/92JB00132